STUDY ON THE WATER SORPTION BEHAVIOR OF HYDROPHOBIC POLYMERS AND ITS APPLICATION TO A CAPACITIVE-TYPE HUMIDITY SENSOR

松口, 正信

https://doi.org/10.11501/3097917

出版情報：九州大学, 1994, 博士（理学）, 論文博士
バージョン：
権利関係：

STUDY ON THE WATER SORPTION BEHAVIOR OF HYDROPHOBIC POLYMERS AND ITS APPLICATION TO A CAPACITIVE-TYPE HUMIDITY SENSOR

松口正信

STUDY ON THE WATER SORPTION BEHAVIOR OF HYDROPHOBIC POLYMERS AND ITS APPLICATION TO A CAPACITIVE-TYPE HUMIDITY SENSOR

Masanobu Matsuguchi

CONTENTS

CHAPTER I

INTRODUCTION

Sorption behaviors on various polymer films are currently being investigated owing to their theoretical and practical significance. Since many applications of polymer materials depend wholly or largely on the sorption behavior, the influence of water on the thermal and mechanical properties of polymers has received considerable attention and the general interaction of water with polymers has been reviewed. The many studies were motivated by the large effect of water on mechanical properties, swelling, glass transition temperature, etc. A number of gas sorption and diffusion measurements have also been performed in the glassy as well as the rubbery state.

The water sorption of a glassy polymer at a given temperature, based on its structure, has not been properly understood. Only the results has been discussed and the reason and the mechanism of such sorption behavior have hardly been discussed so far. One of the most important factors, which affects water sorption ability, seems to be the hydrophilicity of constituent groups of the polymer. In attempting to understand the origins of the differences in hydrophilic character, the relative numbers of atoms present in each polymer that might be expected to form hydrogen bonds in water require consideration. Pauling' s simple hypothesis, that one molecule of water is sorbed per designated polar group, works only for undenatured globular proteins (1,2). More general treatments, based on thermodynamics of mixing and on cohesion parameters, are inadequate for glassy polymers (3). Additional factors must be considered, for example those which relate to molecular packing. In the case of a polymer which has no strong polar group, the sorption site of the water molecule seems to be the free spaces around the polar site of the polymer. Bondi reported on the volume of molecules impenetrable to thermal collision, the so-called van der Waals volume (4). The contributions of the functional group to van der Waals volumes is quite different and the packing density seems to be dependent on the chemical structure of the polymer. Molecular weight is also one of the factors which affects the packing density. Kirgin pointed out that a decrease in molecular weight might result in closer molecular packing in the glassy state and hence to a lower sorptive capacity (5). D. T. Turner studied the influence of molecular weight on the sorption of water by glassy poly(methyl methacrylate), PMMA (6). Samples of PMMA of low molecular weight may take up less water (1.2 wt %) than samples of normally high molecular weight. A low molecular weight sample accommodated only 15 % water in microvoids, as compared with 50% for samples of high molecular weight. From these results, he concluded that closer molecular packing may be effected in samples of low molecular weight in glassy polymers. Further in the respect of molecular packing, cross-linking has produced a marked increase in water sorption in copolymers of methyl methacrylate and dimethacrylate (7-11). The morphology of the materials varies with the level of the cross-linking and the water sorption is dependent on the morphology. It would be interesting to study the morphology of the materials to seek an explanation for this phenomenon.

In order to characterize the sorption behavior on polymer film, the gravimetric method has been used so far. Recently the quartz crystal microbalance (QCM) technique has been widely used to measure the mass change at the molecular level (10,12,13). The QCM is an instrument for accurately measuring the mass change and is useful for observation of the sorption change *in situ* in a state of thin film. Many researchers have also been adopting the measurement of the apparent dielectric constant (14-19). Especially when water vapor is the sorbate, dielectric measurements are believed to be an effective means of determining the macroscopic or microscopic state of the water, because of its strong polarity. Recently, Paley et al. applied the solvatochromic method (20-25) to the characterization of solid polymers. They prepared thin polymer films containing certain media sensitive dyes in these polymeric media and measured the UV-visible absorption spectra of the films (26,27). The obtained empirical parameters might constitute a more comprehensive measure of the characteristics, especially for polarity, or the hydrogen-bonding ability of polymers than the dielectric constant or any other single physical characteristic, since they reflect more faithfully the complete picture of all the intermolecular forces.

The present investigation, therefore, has been undertaken to identify the sorption behavior of water on various polymer thin films that have different chemical structure and morphology, etc. In the first half of the thesis, the discussion was devoted to the problem for clarifying the effect of the characteristics of constituent groups of polymer on the water sorption mechanism and the state of sorbed water. For this purpose, cellulose derivatives, which have a common rigid structural unit and different side groups, were chosen. The solvatochromic method, as well as the gravimetric and the dielectric measurements, was applied to cellulose-water systems and the sorption mechanism and the state of sorbed water in cellulose were discussed. In the latter half, the effect of the cross-linking structure on the water sorption behavior in the hydrophobic polymer, which has a carbonyl group or an imide group in the polymer, was discussed. Finally, the application of these sorption phenomena to a capacitive humidity sensor were mentioned.

CHAPTER II

THEORY

II-I. Water structure in polymers

The water molecule bound within the small space (pore) of a polymer cannot be explained simply by the hydration of hydrophilic site. The structure of water molecule bound in the space were determined by the hydrophobicity of these surfaces, the average pore diameter, etc. The many experiments reported that water inside the pores have a structure and properties which differ from those of a normal liquid phase as shown in Fig. 1. When polymers contain both hydrophobic groups and relatively weak hydrophilic groups, it seems probable, that hydration of the pores in a polymer membrane takes place in sequential steps which occur at very different rates. According to the reported results, the state of water can be classified as follows (28).

(i) Initially, single water molecules were bound to the hydrophilic site by hydration, such as hydroxyl groups, and a monolayer of water molecules is formed. The strength of the bond is large. The molecular motion of water in this region is strongly restricted by hydrophilic groups and the correlation time τ_c has been calculated as 10^{-5} - 10^{-7} s.

(ii) Small weakly-bonded mobile clusters of water molecules grow fairly rapidly on these hydrophilic sites, leaving the hydrophobic regions still in contact with air. This state of water is water weakly interacting with polymer. It is well known that a significant fraction of the water in various wet cellulose acetate membranes does not freeze, probably because of the interaction with the polymer. The nonfreezing bound water is highly mobile compared with ice. Presumably the water, which does not freeze, consists of the small linear clusters, each of which is too small to form an ice nucleus, and which are separated from one another by the continued presence of gas molecules, and regions of unwet hydrophobic surface. Diffusion of such a cluster occurs when one molecule breaks a hydrogen bond with the polymer and simultaneously another makes a bond with the polymer without any change in the water-water bonding. The amount of nonfreezing bound water depends on membrane morphology, that is, it decreases with the increase in the packing density of the polymer within the film. In dense

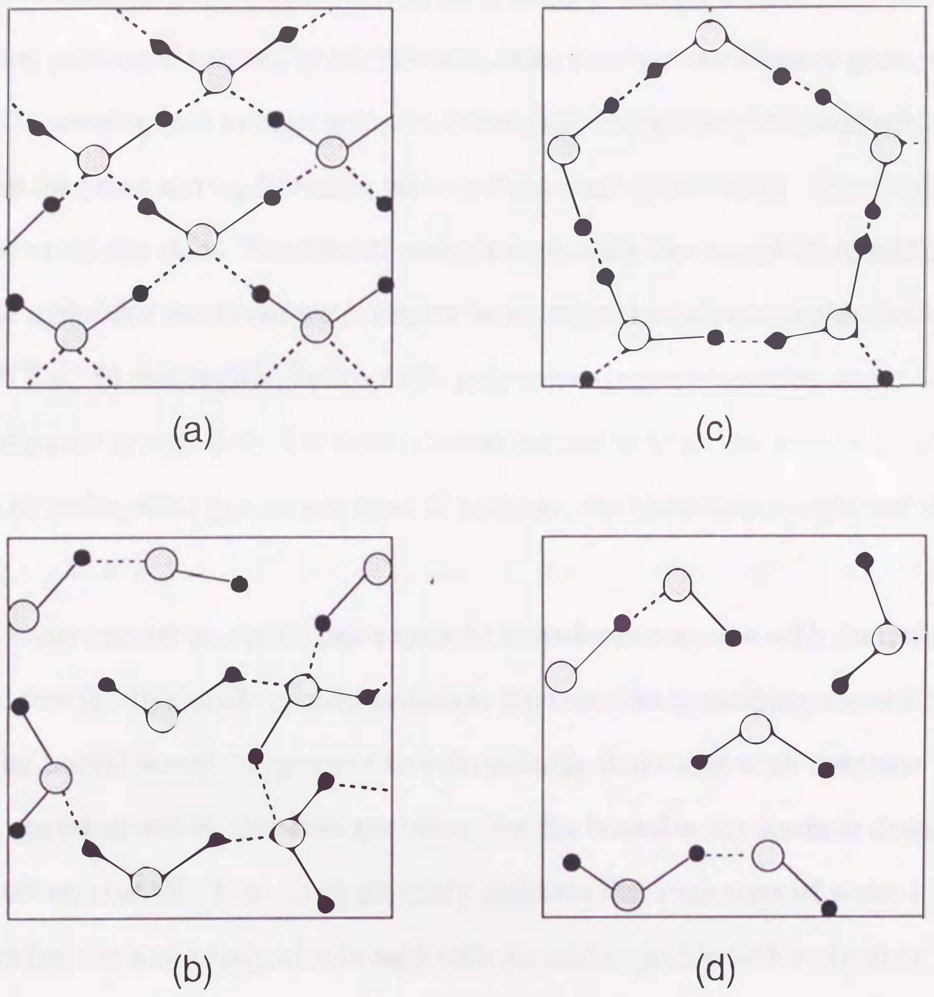
(a) (c)

(b) (d)

Fig. 1. Two dimensional water structure; (a) ice, (b) bulk liquid water, (c) bound water (stretched super cooled), (d) vapor-like water.

films, the extent of polymer-polymer interactions within the polymeric matrix is high, and therefore the macromolecular chains are less accessible to bind water. The τ_c value of water is of the order of 10^{-7} - 10^{-9} s and the molecular motion of water may be affected by the water around hydrophilic groups.

(iii) Following prolonged soaking in liquid water, more slowly water clusters grow, expelling more air and gradually coming into contact with the hydrophobic regions of the surface (stretched water), finally filling the pores and equilibrating with external water (free water). This final equilibration step appears to be extremely slow. This state of water is completely free except for restricting the translational motion. The molecular motion of water cannot be restricted by polymer molecules and τ_c is calculated as 10^{-9} - 10^{-12} s. In this region, hydrophilic polymers are plasticized by water and the molecular motion of polymers is activated. The water content needed to form free water depends on the kind and the number of hydrophilic groups per mole of polymer, the molecular weight and the crystallinity of the polymer.

The free water content decreases faster than the bound water content with decrease in the total water content, and that the free water content is zero in the thin film containing about 12-13 % total water content. The bound water component simultaneously decreases with decrease in the free water component. In other words, this does not mean that the bound water starts to decrease after the free water does not exist at all. This result probably indicates that each state of water in the membrane is not fixed and that the water molecules in each state are exchangeable with each other.

The ratio of water content of each state closely depends on the structure of the membranes. It seems that the ratio of bound water is smaller in the membrane containing large pores than that in the membrane containing small pores. The relation between distribution of pore size and the ratio of free water very weakly interacting with polymer to completely free water is similar to the previous one. Consequently, one may be able to estimate distribution of pore size in thin film.

II-II. Sorption isotherm

Isotherm analysis depends strongly on structural models. A linear increase of the mass sorbed with the activity of the vapor (Henry's law) is not often found in polymer/water systems and is associated with very dilute solutions in which the dissolved water molecules are sufficiently few and far apart for the system to behave as if ideal, i.e., as if a simple random mixture. If the system were in fact ideal, Roult's law would be obeyed, and water and polymer would be infinitely miscible. Brunauer et.al. classified van der Waals adsorption of gases into five different types of isotherm as shown in Fig. 2 (29). An interpretation of the Type I isotherm was given by Langmuir (30). Types IV and V suggest that the complete or almost complete filling of the pores and capillaries of the adsorbent occurs. In the case of the attractive forces between adsorbed gas and adsorbent are greater than the attractive forces between the molecules of the gas in the liquefied state, that is, sorption of water on the hydrophilic polymers which have strong sorption site, the sorption isotherm shows general sigmoidal shape which suggests Type II (31). An isotherm that is linear at low activities and curved upward more rapidly than predicted by Henry's law is a type III isotherm and is sometimes called a Flory-Huggins isotherm (32-34). This case is observed when the attractive forces between adsorbed gas and adsorbent are smaller than the attractive forces between adsorbed gases. The representative isotherm analysis which have been used for the sorption system similar to the present one are as follows.

1. Models for polar systems at high penetrant activities.

The sorption equilibria can be discussed in terms of the solution theory, treating the sorption process as mixing of the solvent and polymer. Inherent in the Flory-Huggins statistics is the idea that there will be some clustering of the water molecules at higher water contents .

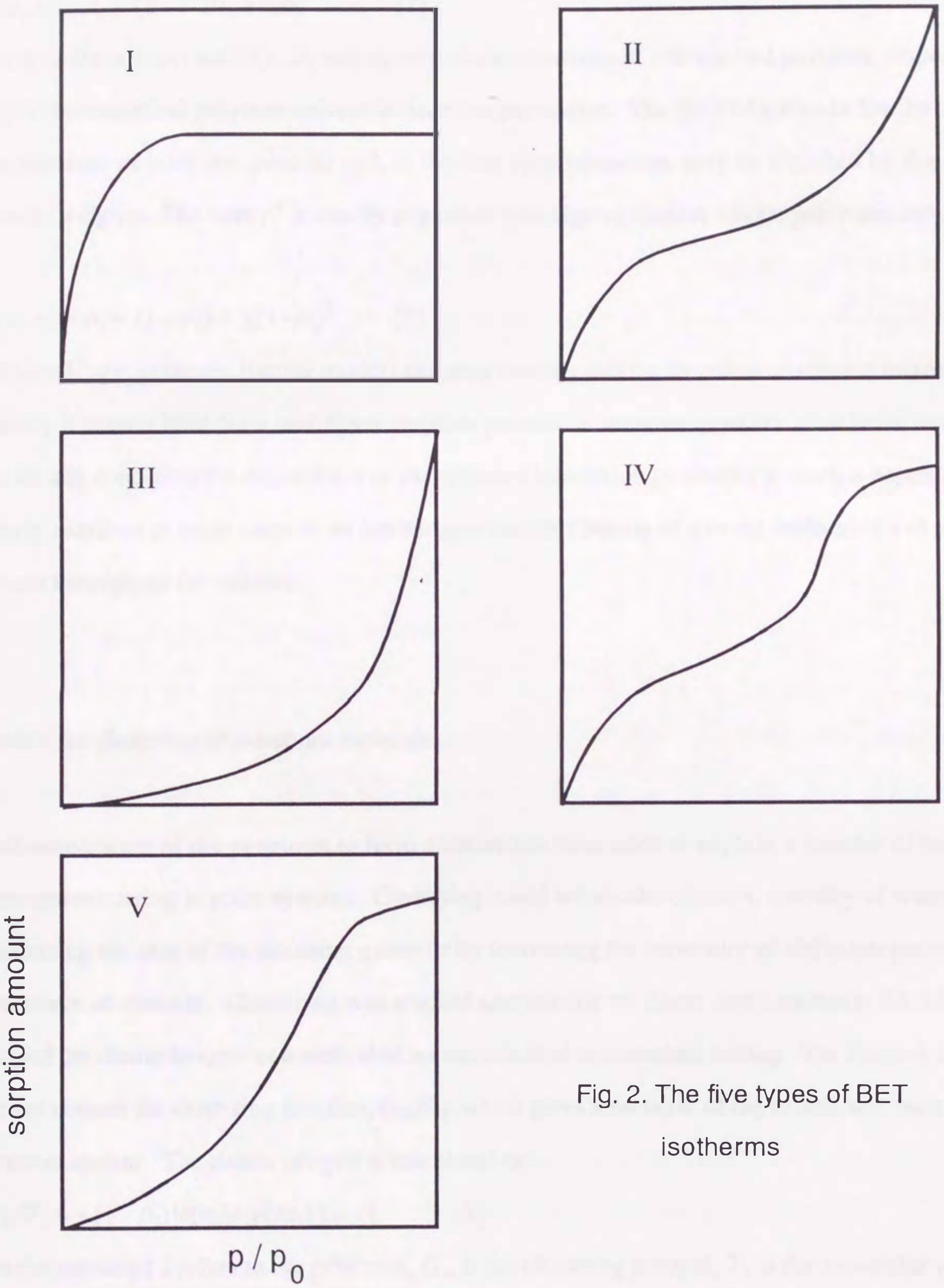

Fig. 2. The five types of BET isotherms

$$\ln a_1 = \ln \rho_1 + (1 - r^{-1})\rho_2 + \chi\rho_2^2 \qquad [1]$$

where a_1 is the solvent activity, ρ_1 and ρ_2 are volume fractions of solvent and polymer, respectively, and χ is the empirical polymer-solvent interaction parameter. The symbol r stands for the ratio of molar volumes of both components and, in the first approximation, may be replaced by the ratio of molecular weights. The term r^{-1} is usually neglected with high-molecular weight polymers and resulted in

$$\ln a_1 = \ln \rho_1 + (1 - \rho_1) + \chi(1-\rho_1)^2 \qquad [2]$$

The Flory-Huggins theory (lattice model) assumes random mixing in polymer-solvent mixtures and obviously it cannot hold for a multilayer sorption process: it remains however of definite interest to point out any concentration dependence of the apparent interaction parameter χ: such a dependence is precisely ascribed in most cases to an inhomogeneous distribution of solvent molecules and polymer segments throughout the solution.

2. Models for clustering of penetrant molecules.

Self-association of the penetrant to form clusters has been used to explain a number of transport phenomena occurring in polar systems. Clustering could reduce the effective mobility of water either by increasing the size of the diffusing group or by increasing the tortuosity of diffusion paths due to the presence of clusters. Clustering was studied specifically by Zimm and Lundberg (35,36), who developed the cluster integral as a method of measurement of non-random mixing. The Zimm-Lundberg treatment defines the clustering function, $G_{11}/\bar{V}_1$, which gives a measure of the cluster size for a binary component system. The cluster integral is calculated as

$$G_{11}/\bar{V}_1 = -(1 - \rho_1)[\partial(a_1/\rho_1)/(\partial a_1)]_{p,T} - 1 \qquad [3]$$

where the subscript 1 refers to the penetrant, G_{11} is the clustering integral, $\bar{V}_1$ is the molecular volume,

ρ_1 the volume fraction of penetrant in the polymer film and a_1 is the activity of penetrant. The activity dependence of $G_{11}/\bar{V}_1$ can be obtained by numerical differentiation of a polynomial fit of the sorption data. For a random solution, the activity is proportional to the volume fraction, and

$$G_{11}/\bar{V}_1 = -1 \qquad [4]$$

When $G_{11}/\bar{V}_1$ is greater than -1, the solute is expected to form clusters. The extent of clustering in solutions is indicated by the extent to which $G_{11}/\bar{V}_1$ exceeds minus one. $\rho_1 G_{11}/\bar{V}_1$, which is another characteristic of the system is related to the mean number of penetrant molecules per cluster, namely, the number of type 1 molecule in excess of the mean concentration of type 1 molecules in the neighborhood of a given type 1 molecule. From Eq. 4, this quantity is obviously $-\rho_1$ for a random solution.

3. Models for gas sorption in glassy polymers.

For systems of a gas and a glassy polymer, sorption isotherms are frequently concave to the pressure axis, approaching linearity at higher pressures. The dual-mode model considers sorption into microvoids, i.e., into the excess of free volume existing in the glass state (37-39). The sorption can be thought of as occurring in two stages, the results of which are added together. At low activities water molecules dissolve in the glass and are preferentially sorbed and arrested in the microvoid structure. The microvoids ultimately reach saturation. This stage is described by a Langmuir tightbinding model and a Langmuir isotherm equation. Exposure to higher activities leads to further simple random solution, described by Henry's law. The isotherm is thus the sum of a Langumir and a Henry's law isotherm. Support for this model of polymer/water interaction has come from many workers. The total concentration C of sorbed penetrant is then given by the dual-mode sorption model:

$$C = C_D + C_H = k_D p + C'_H bp/(1 + bp) \qquad [5]$$

where k_D is the Henry's law constant, *p* the equilibrium penetrant pressure, C_H' the Langmuir capacity constant, and b the Langmuir affinity constant. The solubility of most gases and vapors in a polymer decreases with increasing temperature. This is reflected on the fact that the dual-mode parameters k_D, C_H', and b decrease as the temperature rises. For many systems, C_H' tends to decrease nearly linearly with increasing temperature and vanishes at a temperature very close to the glass transition temperature of the polymer. Equation [5] then reduces to Henry's law.

II-III. Dielectric characterization of the water sorption behavior of polymer thin films

The problem of assessing the true dielectric properties of the adsorbate from the measured properties of the composite system has not been solved completely due to the lack of the knowledge of the electric field at an adsorption site. All methods which have been developed contain some major theoretical assumptions or empirical steps. Among those, the adsorbate + adsorbent system is considered to be analogous to a solution, the components of which follow the Onsager-Kirkwood equation (18). The modified Kirkwood's equation (40) for the permittivity, ε_0 of a binary system is expressed as

$$(\varepsilon_0 - 1)(2\varepsilon_0 + 1) / 9\varepsilon_0 = 4N_1(\alpha_1 + g_1\mu_1^2 / 3kT) / 3 + 4N_2(\alpha_2 + g_2\mu_2^2 / 3kT) / 3 \qquad [6]$$

where N_1 and N_2 are the number of molecules per unit volume, α_1 and α_2 are the polarizabilities, μ_1 and μ_2 are the dipole moments for each other, respectively, k is the Boltzmann constant, T is the absolute temperature, and g, the correlation parameter, is a measure of the local ordering of the dipole. It has a value of one if fixing the position of one dipole does not influence the positions of the rest of the dipoles at all. On the other hand, if fixing one dipole tends to make the neighboring dipoles line up in a parallel direction, the correlation parameter will be greater than one. Similarly, if fixing one dipole tends to line up the neighbors in an antiparallel direction, the correlation parameter will be less than one.

By assuming that the number of polymer per unit volume is hardly dependent on the relative vapor pressure, Equation [6] can be rewritten as follows

$$(\varepsilon_0 - 1)(2\varepsilon_0 + 1) / 9\varepsilon_0 = (\varepsilon_p - 1)(2\varepsilon_p + 1) / 9\varepsilon_p + 4N_w(\alpha_w + g_w\mu_w^2 / 3kT) / 3 \qquad [7]$$

where ε_p is the permittivity of polymer in dry atmosphere and the subscript w, indicates the component of sorbed water.

As water is an extreme case in which the local forces between molecules are very large, the g value may be expected to differ appreciably from unity. When one water molecule is held in a fixed position, and assuming that apart from the four immediate neighbors the surrounding molecules will take up all possible positions at random, we obtain $g = 2.65$. In addition, if the interaction between water molecule and polymer is very large, the apparent value of g is not a constant and varies with the amount of sorbed water. In the case where the water molecule is not associated with the other molecules existing as neighbors, g may be unity. So that, by examining the relationship between the permittivity and the amount of sorbed water, we can obtain information regarding the state of sorbed water on polymer thin films.

For an a.c. electrical field, Eq. [8] is employed instead of Eq. [7]

$$(\varepsilon - 1)(2\varepsilon + 1) / 9\varepsilon = (\varepsilon_p - 1)(2\varepsilon_p + 1) / 9\varepsilon_p + 4N_w(\alpha_w + P(\omega)) / 3 \qquad [8]$$

where $P(\omega)$ indicates the polarization term caused by the orientation of dipole and depends on the applied frequency. When $\omega = \infty$, Equation [8] is rewritten as

$$(\varepsilon - 1)(2\varepsilon + 1) / 9\varepsilon = (\varepsilon_C - 1)(2\varepsilon_C + 1) / 9\varepsilon_C + 4N_2\alpha_2 / 3 \qquad [9]$$

In this case, the dipole moment is zero or becomes ineffective. Consequently, the value of $(\varepsilon - 1)(2\varepsilon + 1) / 9\varepsilon$ measured in the higher frequencies gives the value of the polarizability term and is scarcely dependent on the distortion polarization caused by the intermolecular interaction. By assuming that the low-frequency limit and high-frequency limit of dielectric constant correspond to the dielectric constant observed at 1 kHz and 1 MHz, respectively, the degree of the distortion polarization may be estimated.

In order to clarify the state of sorbed water, it is useful to estimate the dielectric constant of the sorbed water experimentally. We adopted Kurosaki's equation as follows (14),

$$\varepsilon_{app} = \varepsilon_p + V(\varepsilon_{H_2O} - \varepsilon_p), \qquad [10]$$

where ε_{app}, ε_p and ε_{H_2O} are the apparent dielectric constants of the sensor, polymer and sorbed water, respectively. V is the volume fraction of sorbed water calculated from the amount of sorbed water. This formula is obtained, when the frequency is sufficiently high ($\omega\tau \gg 1$) and $\varepsilon_{H_2O} \gg \varepsilon_p$.

Independently, the theoretical estimation of dielectric constant of water were succeeded by Kirkwood.

$$\varepsilon_{H_2O} - n^2 = (3\varepsilon_{H_2O} / (2\varepsilon_{H_2O} + n^2))(4\pi N_0 \mu\mu^* / 3kT) \qquad [11]$$

If we assume that molecule interact with only nearest neighbors, $\mu\mu^*$ is written as

$$\mu\mu^* = \mu^2(1 + z\,\overline{\cos\gamma}), \qquad [12]$$

where z is a number of nearest neighbors and $\overline{\cos\gamma}$ is the average value of $\cos\gamma$ (γ is an angle of adjacent dipoles). Consequently, Eq. [11] is modified as

$$\varepsilon_{H_2O} - n^2 = (3\varepsilon_{H_2O} / (2\varepsilon_{H_2O} + n^2))(4\pi N_0 \mu^2 / 3kT)(1 + z\,\overline{\cos\gamma}). \qquad [13]$$

The equation is also modified by assuming the spherical molecule as

$$\varepsilon_{H_2O} - n^2 = (3\varepsilon_{H_2O} / (2\varepsilon_{H_2O} + n^2))((n^2 + 2) / 3)(4\pi N_0 \mu_v^2 / 3kT)(1 + z\,\overline{\cos\gamma}), \qquad [14]$$

where μ_v is a dipole moment in vacuum. The average number of nearest neighbors are known as almost four in the case of liquid water and $\overline{\cos\gamma}$ is resulted in 1/3. Consequently, we can obtain ε_{H_2O} in liquid water as 64 at 298 K ($N_0 = N_A \times d / W$ ($N_A = 6 \times 10^{23}$, $d = 1$, $W = 18$), $k = 1.4 \times 10^{-16}$, $\mu_v = 1.9 \times 10^{-18}$, $n^2 = 1.77$ and $n^2 << \varepsilon_{H_2O}$). In the case of single water molecule, that is, no interaction between neighboring molecule, the obtained value is 3.19 at 298 K.

II-IV. Solvatochromic characterization of the water sorption behavior of polymer thin films

Usually, chemists have tried to understand solvent effects in terms of the so-called solvent polarity, which is not easy to define precisely or to express quantitatively. Because of the simplicity of electrostatic solvation models, attempts at expressing solvent polarity quantitatively involve mostly physical solvent parameters such as dielectric constant, dipole moment, refractive index, etc. However, this procedure is often inadequate, since it does not take into account specific solute-solvent interactions such as hydrogen-bonding , electron-pair donor (EPD) - electron-pair acceptor (EPA), and solvophobic interactions. Hence, from a more practical point of view, it seems reasonable to understand solvent polarity in terms of the overall solvation capability of a solvent for reactants and activated complexes as well as for molecules in the ground and excited states, excluding solute-solvent interactions such as protonation, oxidation, reduction complexation, etc., which may lead to a chemical change of the solute. This overall solvation capability depends on all possible-specific and nonspecific-intermolecular forces between solute and solvent. Obviously, solvent polarity thus defined cannot be described by a single physical solvent parameter. The lack of comprehensive theoretical expressions for the calculation of solvent effects, and the inadequacy of defining solvent polarity in terms of simple physical characteristics, has led to the introduction of empirical parameters of solvent polarity.

It was observed long ago, during comparison of the absorption spectra of a substance in the gas phase and in solution, that the solvent causes a change in the position, intensity, and shape of the bands. This phenomenon was termed "solvatochromism". The reason for the solvent-dependence of the wave number of the absorption and emission of light is the difference in the stabilization of the ground state and excited states by intermolecular forces, which can lead to an increase or decrease in the excitation energies. The most important of interaction between molecules with a permanent dipole in the ground state and non-polar or polar solvent molecules, apart from hydrogen bonding, are polarization forces (electrostatic directional and inductive forces between dipoles and induced dipoles). The extent of the interaction, and hence of the spectral shift, depends both on the polarity of the dye and on that of the solvent, and is especially large in the case of intramolecularly ionic dyes, such as merocyanines or the pyridinium-N-phenol betaines. In dyes of this type, an electron-donating group is joined to an electron-accepting group *via* a conjugated system. The excitation is associated with a charge transfer between the two groups, resulting in an appreciable change in the magnitude and direction of the dipole moment in the excited state. Based on the assumption that particular, carefully selected and well understood spectral absorptions may serve as suitable model processes, various empirical solvent polarity scales have been developed. The first to suggest that solvatochromic dyes might be used as indicators of solvent polarity was Brooker in 1951 (41), but Kosower was the first to set up a real spectroscopic solvent polarity scale in 1958 (20). This was called the Z-scale and used the intermolecular charge-transfer absorption of.1-ethyl-4-methoxycarbonylpyridinium iodide as solvent-sensitive reference process. Kosower suggested that spectral shifts of strongly absorbing solutes in various solvents might be used to establish a scale of solvent polarity. It is generally recognized that the effect of a solvent on the spectrum of a solute is the resultant of a large number of factors - static factors such as interaction between solvent and solute permanent dipoles, dynamic factors such as dispersion forces, solvent sorting in the case of mixed solvents, and specific interactions such as hydrogen bonding between solute and solvent.

1. E_T - values of pyridinium N-Phenolbetaines.

The pyridinium N-phenoxide betaine dye (2,6-diphenyl-4-(2,4,6-triphenylpyridinio) phenolate) was proposed by Dimroth, Reichardt, et.al. as a new UV/Vis spectroscopic indicator of solvent polarity. The dye overcome some practical limitations of other solvatochromic reference molecules by virtue of its exceptionally large negative solvatochromism (21). The E_T values calculated from

$$E_T \text{ / kcal mol}^{-1} = hc\bar{\nu}N_A = 2.8591 \text{ X } 10^{-3}\bar{\nu}_{\max} \text{ / cm}^{-1} = 28591 / \lambda_{\max} \text{ / nm}^{-1}, \qquad [15]$$

where h is Planck's constant, c is the speed of light in a vacuum and N_A is Avogadro's number, for the pyridinium N-phenolbetaine used as the test substance provide an excellent characterization of the polarity of solvents, owing to the extraordinarily large displacement of the solvatochromic band. This displacement of a solvatochromic band observed is the largest so far known : the long-wave band is situated at 810 mμ (E_T = 35.3 kcal/mole) in diphenyl ether and at 453 mμ (E_T = 63.1 kcal/mole) in water corresponding to a hypsochromic solvatochromic band lies in the visible region of the spectrum, it is even possible to make a visual estimation of the polarity of a solvent. This outstanding negative solvatochromism stems from the unequal, differential solvation of the electronic ground and excited state of dye with increasing solvent polarity (Figure 3). The solvent-mediated stabilization of the highly dipolar, zwitterionic ground state of dye, relative to its less dipolar excited state, results from the following properties of the betaine molecule: (a) it exhibits a large permanent dipole moment, suitable for the registration of dipole-dipole and dipole-induced dipole interactions; (b) it possesses a large polarizable π-electron system, suitable for the registration of dispersion interactions; and (c) with the phenoxide oxygen atom it has a highly basic EPD centre, suitable for interaction with Bronsted acids (through H-bonding) and Lewis acids (through EPD-EPA bonding). The positive charge of the pyridinium moiety is delocalized and sterically shielded. Therefore, the CT absorption of dye depends strongly on the electrophilic solvation power of the solvents, i.e. on their hydrogen-bond donor (HBD) ability and Lewis acidity (= EPA behavior), rather than on their nucleophilic solvation capability (=EPD behavior). In stronger acidic solvents, dye is protonated and the solvatochromic CT absorption band disappears (reversibly). A high $E_T(30)$ value corresponds to high solvent polarity.

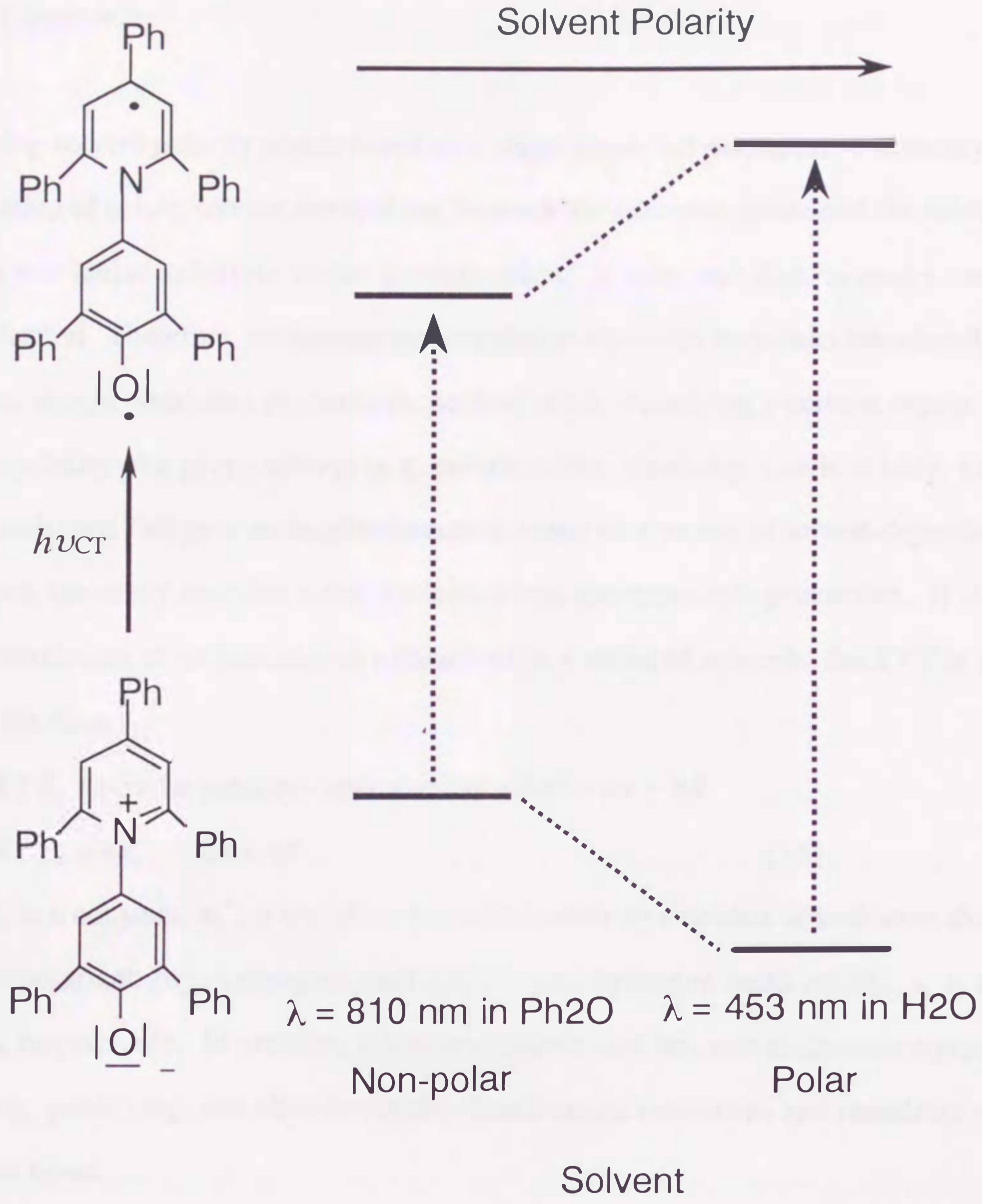

Fig. 3. The solvent-mediated stabilization of electronic state

2. The KAT approach.

In applying solvent polarity scales based on a single empirical parameter, it is tacitly assumed that the combination of solute-solvent interactions between the reference solute and the solvent is the same as with the particular substrate under consideration. It turns out that, in many cases, this is an oversimplification. Therefore, multiparameter correlation equations have been introduced, which consist of up to four single empirical parameters, each of them measuring a certain aspect of the overall solvation capability of a given solvent (e.g. polarizability, dipolarity, Lewis acidity, Lewis basicity) (22-24). Kamlet and Taft gave an empirical equation based on a variety of solvent-dependent phenomena (XYZ), which are many reaction rates, equilibria and spectroscopic properties. If the XYZ is the absorption maximum of an indicator dye dissolved in a series of solvents, the XYZ is given through equation of the form

$$
\begin{aligned}
XYZ &= XYZ_0 + \text{solvent polarity - polarizability effect} + a\alpha + b\beta \\
&= XYZ_0 + s\pi_1^* + a\alpha + b\beta \qquad [16]
\end{aligned}
$$

where XYZ_0 is a constant, π_1^*, α and β are the solvent scale by selection of indicators that are sensitive to dipolarity/polarizability, hydrogen bond basicity and hydrogen bond acidity, s, a and b are the coefficients, respectively. In practice, it has been shown that this solvatochromic equation is capable of correlating, predicting, and elucidating physicochemical properties and reactivity parameters of many diverse types.

3. Characterization of polymers by solvatochromic method.

Paley *et.al.* have shown that it is possible to determine the above parameters for solid polymers by measuring the UV/Vis absorption spectra of a series of four dyes dissolved in the polymers (26,27).

Dipolarity/polarizability, π_1^*, is determined from the longest wavelength UV-visible absorption band maximum (the solvatochromic band) of 4-nitro-N,N-dimethylaniline (**1**) in the polymer, eq.[17] (24).

$$\pi_1^* = 8.006 - 0.2841\ \bar{\nu}_{max}(\mathbf{1}) \qquad [17]$$

In this equation, and all those following, $\bar{\nu}_{max}$ values are given in units of 10^3 cm.

Hydrogen bond basicity, β, is determined from the longest wavelength absorption maxima in the polymer of 4-nitroaniline (**2**) (a good hydrogen bond acid) and 4-nitro-N,N-dimethylaniline (**1**) (a poor hydrogen bond acid), eq.[18] (22).

$$\beta = (0.984\ \bar{\nu}_{max}(\mathbf{1}) - \bar{\nu}_{max}(\mathbf{2}) + 3.40) / 2.67 \qquad [18]$$

Hydrogen bond acidity, α, is determined from the longest wavelength absorption maxima of 4-nitroanisole (**3**) (a poor hydrogen bond base) and Reichardt's betaine, 2,6-diphenyl-4-(2,4,6-triphenylpyridinio)phenolate (**4**) (a good hydrogen bond base), eq. [19] (23).

$$\alpha = (\bar{\nu}_{max}(\mathbf{4}) + 1.873\bar{\nu}_{max}(\mathbf{3}) - 74.58) / 6.24 \qquad [19]$$

The E_T value of the polymer is computed from the *longest wavelength absorption maximum* of Reichrdt' s dye in the polymer, eq. [15].

The parameters obtained make chemical sense in that they are similar to those found for liquid solvent models. Further Paley et.al. have demonstrated that relative humidity can have significant effects on the solvatochromic parameters (α and E_T). Since these parameters have been shown to relate to sorption properties of small molecules, they presumably also relate to the sorption properties of the polymers as well. The polymer solvatochromic parameters should prove useful in predicting and understanding the solubility and sorption properties for interaction of polymers with gaseous, liquid, and solid solutes and with bulk liquid solvents. However, we have to note that there are some limitations of the solvatochromic methodology. First, the dyes must be soluble in the polymer. Otherwise aggregates of dye molecules are formed whose UV/vis spectra reveal nothing about properties of the polymers. Second, the polymer and dye must be soluble in some volatile solvent to permit coating of the polymer onto the substrate. Paley et.al. reported that dissolving dyes in the monomers and initiating polymerization usually destroys the chemical integrity of the dye molecules. Thus it appears, at this point, that direct application of the solvatochromic method to polymers is restricted to those polymers that are capable of solution in solvents that also dissolve dye molecules **1-4**.

CHAPTER III

EXPERIMENTAL

1. Materials

Various kinds of polymers, such as cellulose derivatives, methacrylate derivatives and polyimide derivatives, were used in this study for characterizing the sorption behavior of water molecule in polymer thin films. Four kinds of dyes were also used for optical measurement. Detailed description of materials used in the present study were shown in the corresponding section in CHAPTER IV.

2. Preparation of measuring device

The device for electrical measurement was prepared as follows. Each polymers were spin coated (*ca.*2~3 μm in thickness) on a glass substrate which had a platinum electrode (thousands angstroms in thickness) deposited by RF sputtering technique. The film was dried and/or polymerized at elevated temperature. After preparing the polymer thin film, the upper gold electrode (*ca.*100 Å in thickness) was prepared by vacuum evaporation technique and the area of electrode of devices was 2 × 4 mm. The structure of the device is illustrated in Fig. 4.

For the measurement of the amount of sorbed water, the thin films were formed on the quartz oscillator (4 MHz) in a similar manner mentioned above. The oscillator had two Ag electrodes in both sides (Fig. 5).

The element for optical measurement was prepared as follows. The composite solution of the polymer and dye was coated on the interior side of the special quartz cell with a syringe needle as shown in Fig. 6.

A detailed description of procedure was described in each corresponding section.

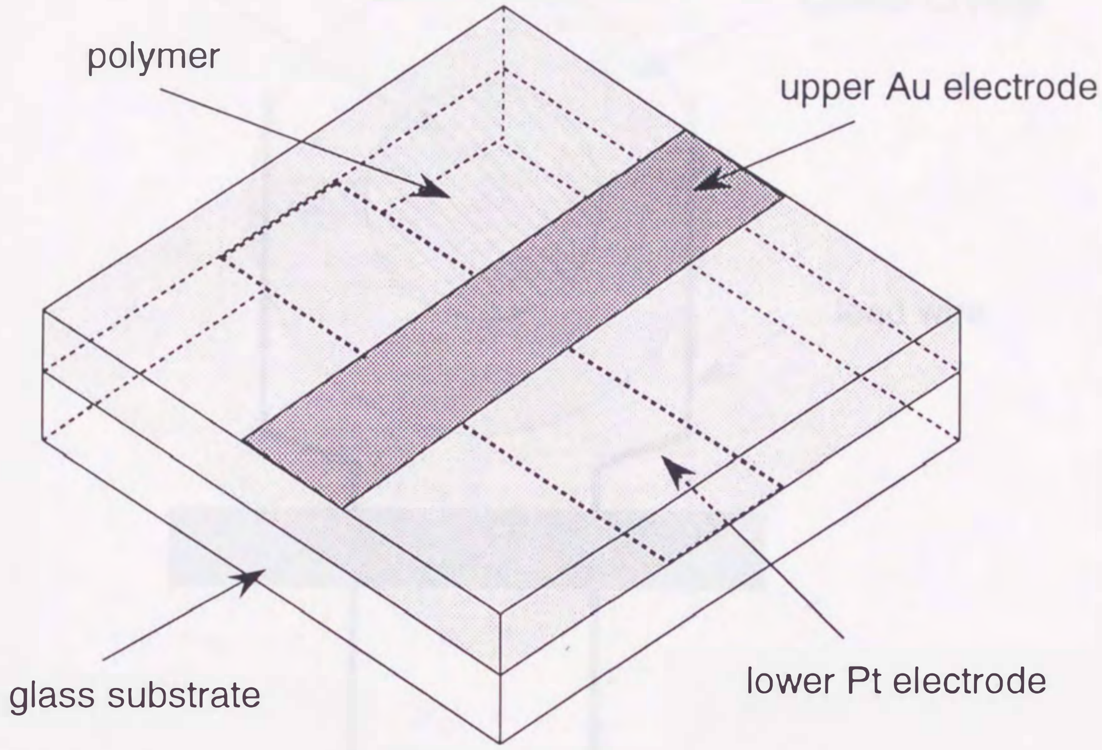

Fig. 4. The structure of the device for dielectric measurement.

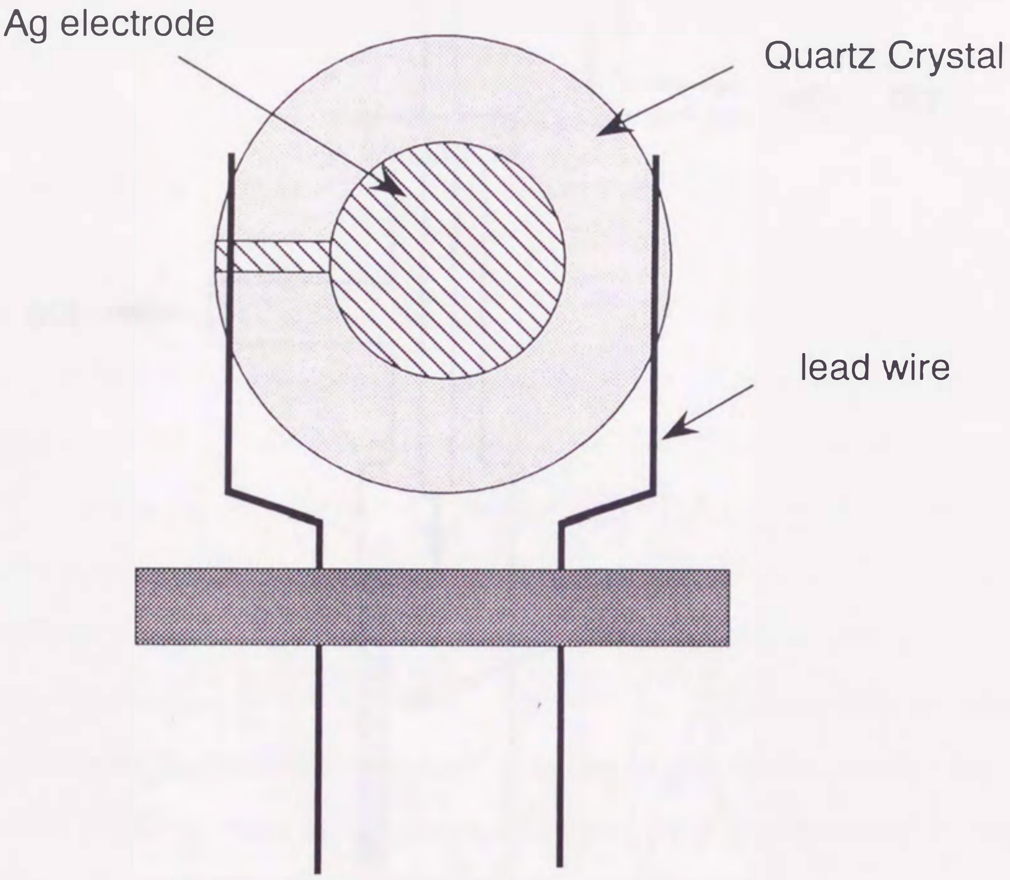

Fig. 5. The structure of quartz oscillator.

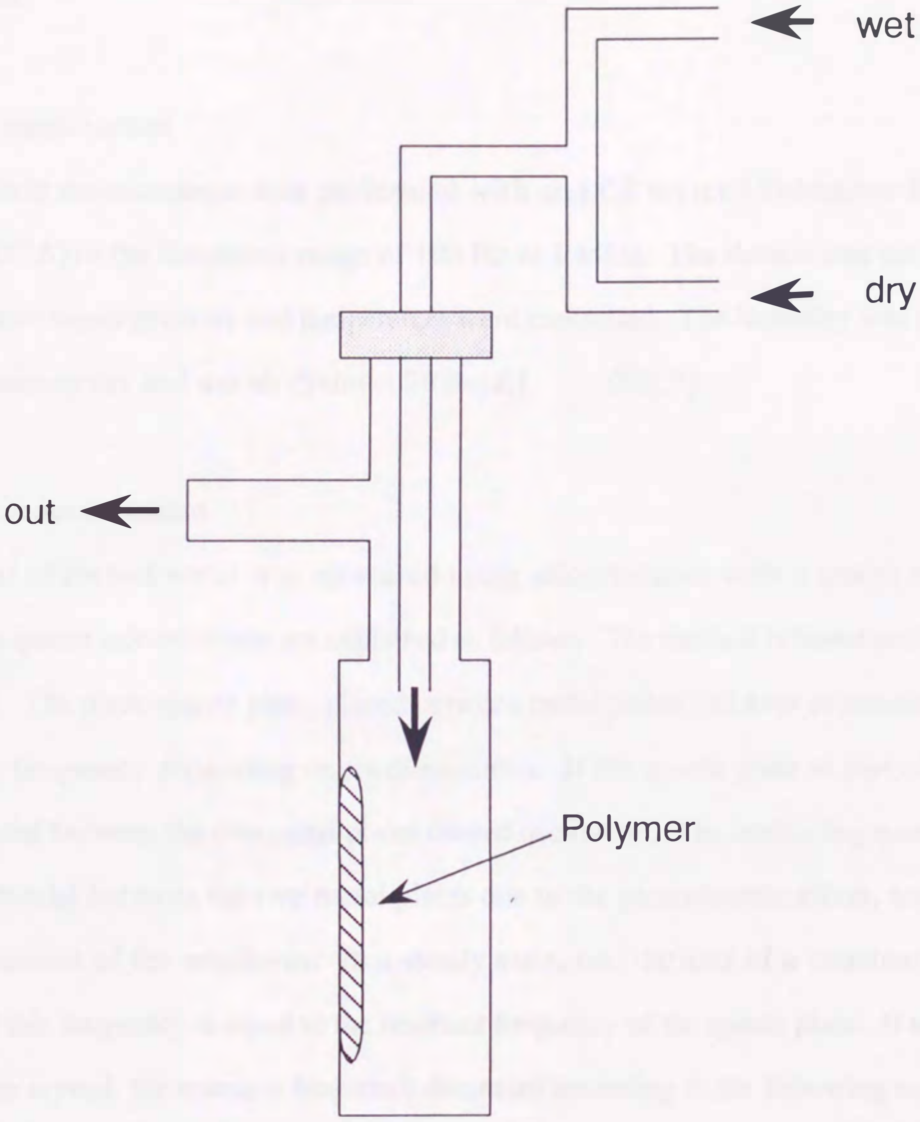

Fig. 6. The structure of special quartz cell for optical measurement.

3. Measurement

3-1. Dielectric measurement

The dielectric measurement was performed with an LCZ meter (Yokogawa-Hewlett-Packard 4276A and 4277A) in the frequency range of 100 Hz to 1 MHz. The device was set in the vessel in which the relative vapor pressure and temperature were controlled. The humidity was thermostatically controlled by mixing dry and wet air (Shinyei SRH-1R). (Fig.7)

3-2. Gravimetric measurement

The amount of sorbed water was measured using microbalance with a quartz oscillator. The principle of the quartz microbalance are explained as follows. The method is based on the piezoelectric effect (42,43). The piezo-quartz plate, placed between metal plates and kept at constant temperature, has a resonant frequency depending on its dimensions. If the quartz plate is part of an oscillating circuit, a potential between the two metal plates caused oscillation. The oscillating quartz generates an alternating potential between the two metal plates due to the piezoelectric effect, and this potential controls the current of the oscillator. In a steady state, oscillations of a constant frequency are generated, and this frequency is equal to the resonant frequency of the quartz plate. If some material is deposited on the crystal, the resonant frequency decreases according to the following equation:

$$\Delta f = - (f^2 m) / (NA\rho) \qquad [20]$$

where f is the resonant frequency of the quartz crystal, N is the frequency constant (for an AT-cut quartz = 1670 kHz), ρ is the density of quartz (=2.648 g.cm^3), A is the surface area of the quartz plate. Consequently the linear relationship between the mass added onto the crystal surface and the change in its frequency can be derived.

The AT cut quartz crystal of 4 MHz resonant frequency was used in the present study. Both sides of the crystal were coated by a silver by the evaporation technique. The polymer coated crystal was set

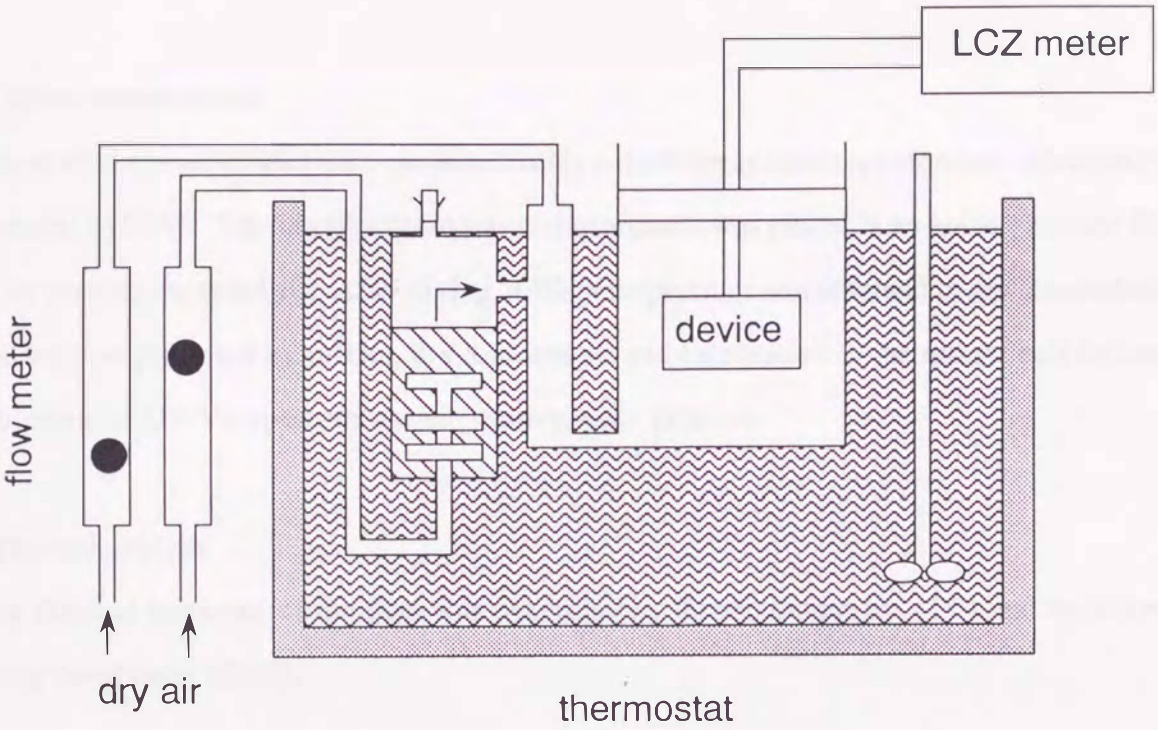

Fig. 7. The apparatus for preparing certain relative vapor pressure.

in a small cell which was prepared in our laboratory. The amount of sorbed water was calculated from the variation in oscillating frequency of the QCM with universal counter (ADVANTEST, TR5822). The relative vapor pressure was thermostatically controlled by mixing dry and wet air. The principle of this method is the same as that of equipment shown in Fig. 7.

3-3. Optical measurement

The optical characteristics were measured using a diode array spectrophotometer (Hewlett-Packard Co., model 8452A). The thin film coated special quartz cell was placed in an holder, and the film was dried by passing the dried air. After drying, a UV/Vis spectrum was obtained in dry atmosphere. The humid air was prepared by mixing dry and wet air and introduced in the quartz cell followed by measurement of UV/Vis spectrum at each relative vapor pressure.

3-4. Thermal analysis

The thermal behavior of the film was examined by thermogravimetry (TG) and by differential scanning calorimetry (DSC).

CHAPTER IV

RESULTS AND DISCUSSION

IV-I. Effect of the polar group on the water sorption behavior of the cellulose thin films

1. Introduction

The amount of sorbed water depend on not only the polarity but also the morphology of the film. Further, as mentioned in CHAPTER II-I, the water bound within the small space of a polymer, which contain hydrophobic groups and relatively weak hydrophilic groups, have a structure which differ from those of a liquid phase (Fig. 1). However, various factors which affect the water sorption behavior of such hydrophobic polymers are hardly revealed. In order to clarify the effect of polarity of the film on the water sorption behavior, it is needed to use the series of polymers with common rigid structure unit but different polar group. Cellulose derivatives seems to be appropriate for this purpose and are perhaps the most extensively investigated polymer that have mixed hydrophilic / hydrophobic surfaces. Cellulose have up to three ester and/or ether groups per glucose monomer. Consequently, their hydrophilic centers, to which water hydrogen bonds, are ester, ether and a few gluconic acid groups. There had been studied on the water sorption behavior and the states of the sorbed water in the cellulose derivatives from the various point of view (44-53). However, there are few chemical discussion based on their chemical structure such as the kind or the content of substituted groups.

The object in this study is the clarification of water sorption behavior in cellulose derivative thin films on the basis of sorption isotherm, dielectric and solvatochromic measurements. In order to reveal some factors affect on the sorption behavior, we used four kinds of cellulose derivatives that the content of hydrophilic groups is known. The relation between the chemical structure of cellulose and the water sorption behavior is discussed.

2. Experimental

2-1. Materials

Cellulose acetate (CA 39), cellulose acetate butyrate (CAB 38), cellulose acetate propionate (CAP 48) and ethyl cellulose (EC) were used. These cellulose were chosen because of their similar hydroxyl contents. Their chemical structures are shown in Fig. 8.

For the optical measurement, four kinds of dyes, 4-nitro-N,N-dimethylaniline (**1**), 4-nitroaniline (**2**), 4-nitroanisole (**3**) and 2,6-diphenyl-4-(2,4,6-triphenylpyridinio) phenolate (**4**) were used as indicators. Their chemical structures are illustrated in Fig. 9, respectively.

2-2. Preparation of measuring device

For dielectric measurement, sandwich type devices were prepared. One gram of cellulose derivatives were dissolved in 10 ml of acetone. Thin films were prepared by spin coating on a platinum-coated glass. The prepared film was dried at 50 ℃ in vacuo for obtaining amorphous film, because it is well known that the water sorption occurred only in the amorphous regions and sorption ability of cellulose is linearly related to the fraction of amorphous phase (44, 48). After preparing the polymer thin film, the upper gold electrode was prepared by a vacuum evaporation technique. Film thickness was several micrometers. The structure was already shown in Fig. 4.

For the measurement of optical characteristics, 1 g of polymers were dissolved in 10 ml of acetone, respectively. The indicators required to determine the solvatochromic parameters were then dissolved in these solutions in several weight ratios of polymer and indicator. The composite solution of the polymer and indicator was coated on the interior side of the special quartz cell with a syringe needle as shown in Fig. 6. The film was dried at 50 ℃ in vacuo in the glass tube oven for 30 min.

Thin film was also coated on a quartz crystal with silver electrode (4MHz) for the measurement of the amount of sorbed water as shown in Fig. 5.

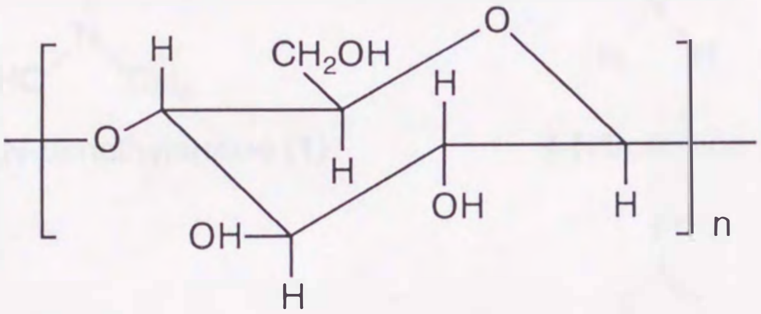

CA 39 $[C_6H_7O_2(OH)_{0.5}(OCOCH_3)_{2.5}]_n$

CAP 48 $[C_6H_7O_2(OH)_{0.6}(OCOCH_3)_{0.16}(OCOC_2H_5)_{2.24}]_n$

CAB 38 $[C_6H_7O_2(OH)_{0.36}(OCOCH_3)_{0.9}(OCOC_3H_7)_{1.74}]_n$

EC $[C_6H_7O_2(OH)_{0.5}(OC_2H_5)_{2.5}]_n$

Fig. 8. Chemical structure of cellulose derivatives.

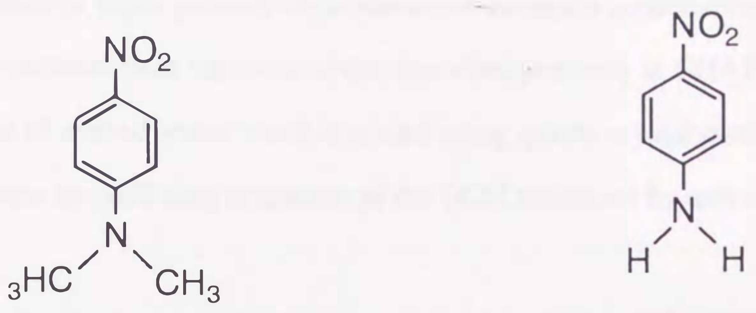

4-Nitro-N,N-dimethylaniline (**1**)   4-Nitroaniline (**2**)

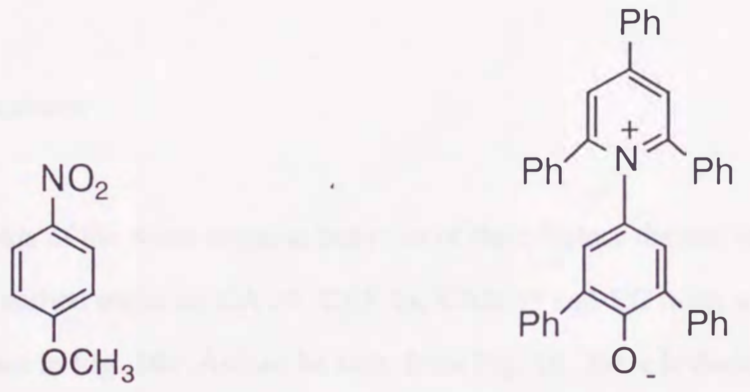

4-Nitroanisole (**3**)   2,6-diphenyl-4-(2,4,6-triphenylpyridinio) phenolate (**4**)

Fig. 9. Chemical structure of four kinds of indicator dyes.

2.3 Measurement

The dielectric measurement was performed with an LCZ meter in the frequency range of 100 Hz to 1 MHz. The relative vapor pressure dependences of electrical capacitance were measured.

The optical measurement are same as that described precisely in CHAPTER III.

The amount of sorbed water was calculated using quartz crystal oscillating microbalance (QCM) from the variation in oscillating frequency of the QCM measured by universal counter.

Further details of experimental procedures were described in CHAPTER III.

3. Results and discussion

3-1. Sorption analysis of the water sorption behavior of the cellulose derivatives

The amount of sorbed water on CA 39, CAP 48, CAB 38 and EC films were measured. Sorption isotherms are shown in Fig. 10. As can be seen from Fig. 10, there is decidedly more water sorbed by CA 39 film than other cellulose films in a whole relative vapor pressure region. For CA 39, which sorb more water, the sorption isotherm curve was similar to type II shown in Fig. 2. The shape of the sorption curve changed gradually from type II to type III with decreasing the sorption ability of the cellulose. As mentioned in CHAPTER II, type II isotherm is observed when water sorb in the hydrophilic polymers which have strong sorption site. As the attractive forces between adsorbed gas and adsorbent are smaller than the attractive forces between adsorbed gases, type III curve is observed. This isotherm that is linear at low activities and curved upward more rapidly than predicted by Henry's law is sometimes called as a Flory-Huggins isotherm. The amount of sorbed water observed in the desiccation process was larger than that in the humidification process as shown in Fig. 11. The difference of the sorbed water measured in both processes (which are called as hysteresis) was larger

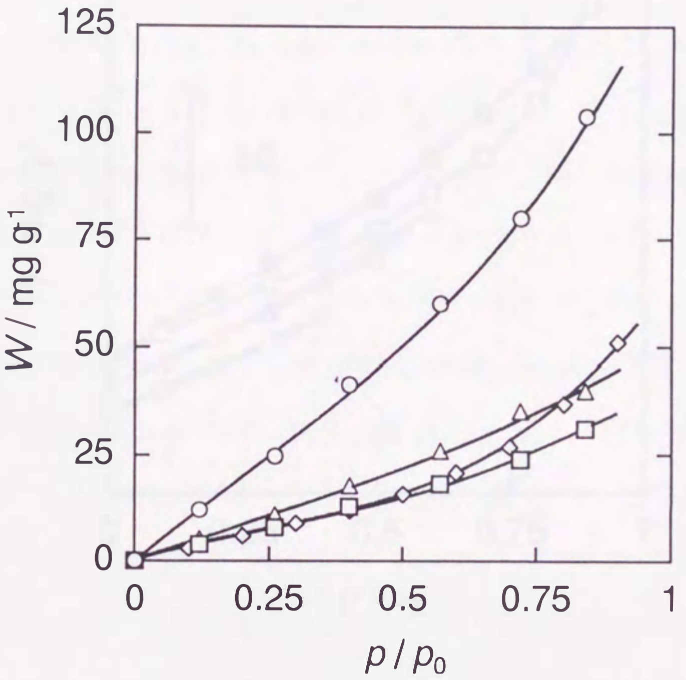

Fig. 10. Sorption isotherms of cellulose measured at 30 ℃;

○) CA 39, △) CAP 48, □) CAB 38 and ◇) EC.

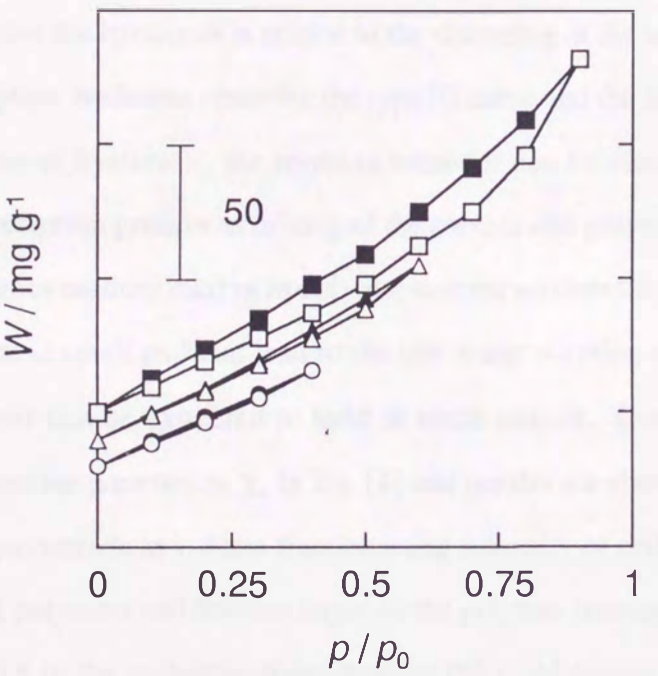

Fig. 11. Water sorption isotherm for CA 39 measured at 30 ℃; (○,●) within p / p_0 =0.4, (△,▲) within 0.6 and (□,■) within 0.9; Open symbols, humidification: Closed symbols, desiccation.

for CA 39 film than that for CAB 38. Despite the lower sorption ability, EC had a larger hysteresis. For CA 39, the water sorption isotherm observed in the desiccation process was strongly depended on the history of exposure to a humid atmosphere as shown in Fig. 11. While any distinct differences of water sorbed in the humidification processes started from 0 %RH were not confirmed, the amount of water observed in the desiccation process increases with increase in the highest humidity of exposure. This result suggest that the hysteresis is related to the clustering of the sorbed water.

Since the sorption isotherms resemble the type III curve and the formation of clusters is expected from the observation of hysteresis, the sorption behavior can be discussed in terms of the solution theory, treating the sorption process as mixing of the solvent and polymer. The Flory-Huggins theory (lattice model) assumes random mixing in polymer-solvent mixtures in solution. Since the number of specific sorption site is small and that lead to the low water sorption ability, the random sorption of water in the polymer can be expected to hold in some degree. Consequently, we estimated the polymer-water interaction parameters, χ, in Eq. [2] and results are shown in Fig. 12. Here data were transformed from gravimetric to volume fraction using a density of cellulose of 1.2. The values of χ, were positive for all polymers and became larger as the polymer became hydrophobic. The value of χ was reported as 1.18 in the cellulose-water system (52). Although the chemical structure is not specified in that literature, it seems that the results obtained in this work are reasonable value. For CA 39, which sorb more water, the interaction parameter is a slightly increasing function of the water content and approaches constant value at high water vapor pressure. In the case of more hydrophobic polymer except for EC, the value of χ is almost constant over the whole water contents. The value of χ, is related to the differences between the water binding energies, which decrease in the order of site binding (negative values of χ,) > indirect binding > water-water interaction in bulk water. The results shown in Fig. 12 suggest that the water is loosely bound to the polymer. It is natural that the more hydrophobic polymer has larger positive value of χ. The reason for the slightly increasing of χ for CA 39 can be explained in terms of predominant site binding at low water concentration followed by

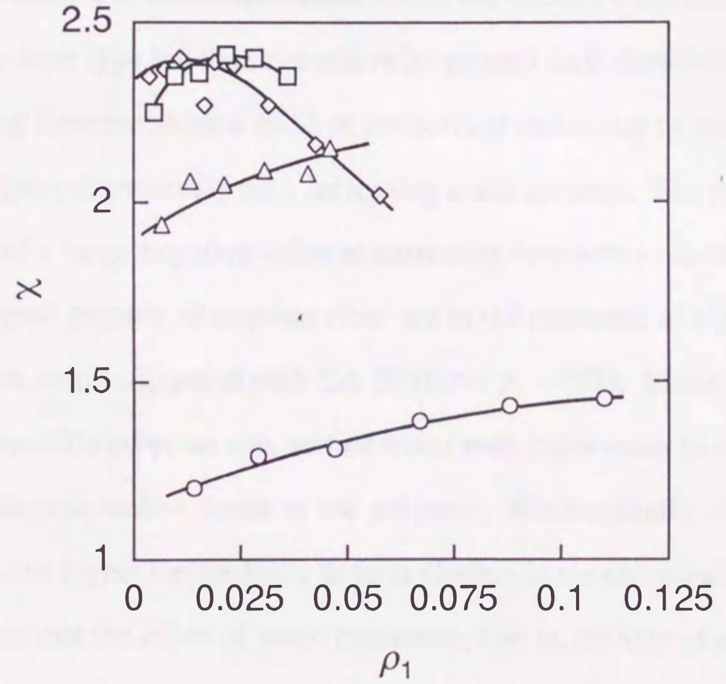

Fig. 12. Dependence of Flory-Huggins parameter, χ, on volume fraction of sorbed water; (○) CA 39, (△) CAP 48, (□) CAB 38 and (◇) EC.

nonspecific and slightly looser indirect binding for higher one. It is noteworthy that the value of χ decreased for EC.

Another method to estimate the tendency of molecules to cluster is that the clustering function developed by Zimm and Lundberg used with binary system in equilibrium. The calculated variations using Eq. [3] of the clustering function versus water volume fraction ρ_1 are plotted in Fig. 13. The clustering function G_{11}/V_1 is an increasing function of the water concentration from the large negative value to the positive value. For an ideal solution where the solvent excludes its own volume to the other molecules of the same type but does not otherwise perturb their distribution, $G_{11}/V_1 = -1$; higher values of the clustering function show a trend of the solvent molecules to cluster. It seems that the sorption process changes progressively with increasing water content. The polymer which had low sorption ability showed a large negative value at extremely low water concentration. This can be explained due to the small number of sorption sites, not to the existence of highly specific sites. EC showed a large positive value compared with CA 39 above $\rho_1 = 0.02$. Since hydrophobic polymer does not have highly specific sorption site, sorbed water molecules seem to be the relatively strong hydrogen bonding acceptor and/or donor in the polymer. Consequently, the more the cellulose becomes hydrophobic, the higher the tendency to form clusters at the same water contents. It must be taken into consideration that the effect of steric hindrance, that is, the size of substituted group. The adequate spaces are needed to form the cluster. It is well known that EC have a high trend of the water to cluster and the obtained result is consistent with the reports (49, 52). In describing order of the polarity by sorption data, the series represents the order of hydrophilicity, with ester groups per unit volume increasing from butyrate to acetate inserted in the cellulose derivatives. This was reflected in terms of an orderly decrease in χ and increase in saturation sorption. However, ethyl group affected on the sorption behavior differently from ester groups especially for clustering tendency. Trend in the clustering appears to be related to the hydrogen bonding propensity of the polar groups in the polymer as well as to the concentration of polar groups.

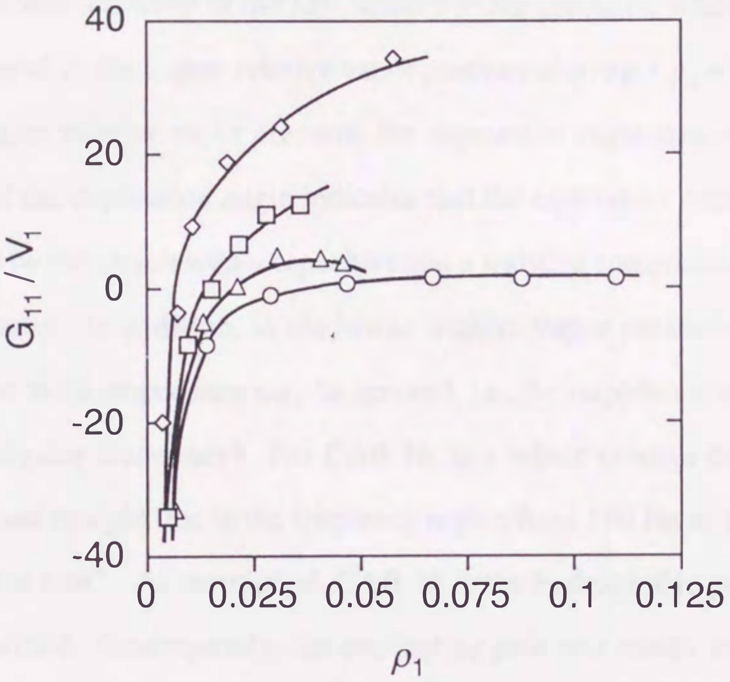

Fig. 13. Dependence of clustering function, G_{11} / V_1, on the volume fraction of sorbed water; (○) CA 39, (△) CAP 48, (□) CAB 38 and (◇) EC.

3-2. Dielectric study on the water sorption behavior of the cellulose derivatives

Since water has large dielectric constant value, the apparent dielectric constant of polymer seems to be enhanced by the sorption of water. Consequently, the dielectric measurement was performed.

First, complex impedance has been employed to analyze the impedance measurements because it seems that the impedance consists of resistive and capacitive components. Complex impedance plots were shown in Fig. 14 for CA 39. In the frequency region from 100 Hz to 1MHz, the quasi straight line past the origin was observed in the low relative vapor pressure, while the semicircles past the origin were confirmed in the higher relative vapor pressure above p / $p_0 = 0.7$. For the semicircles observed in the higher relative vapor pressure, the depression angle was estimated to be ~7 degree. This small value of the depression angle indicates that the equivalent circuit of this condenser-like device is expressed by the circuit with a capacitive and a resistive component inserted in parallel to the capacitive component. In addition, in the lower relative vapor pressure, the contribution of the resistive component to the impedance may be ignored, i.e.,the impedance was approximated to $1/\omega C$ (ω is the applied angular frequency). For CAB 38, in a whole relative humidity, the results were represented by a quasi straight line in the frequency region from 100 Hz to 1 MHz and the impedance was approximated to $1/\omega C$. As mentioned, CAB 38 is the hydrophobic polymer and sorbed water seems to be delocalized. Consequently, the conducting path was hardly formed and resulted in the formation of ideal condenser.

The relationship between the electrical capacitance and relative vapor pressure was examined. In Fig. 15, the relative vapor pressure dependences of the capacitance observed at 100 kHz were shown. The value of C / C_0 (since the capacitance is affected by the film thickness, the ratio of capacitance at a certain relative vapor pressure to that capacitance at p /$p_0 = 0$ was adopted for comparison) is plotted on the ordinate. The value increased with increase in the relative vapor pressure. This is because of the sorption of water molecule, which has large dielectric constant. Consequently, dependence of the C / C_0 on W was examined and is shown in Fig. 16. The almost identical relation was observed except

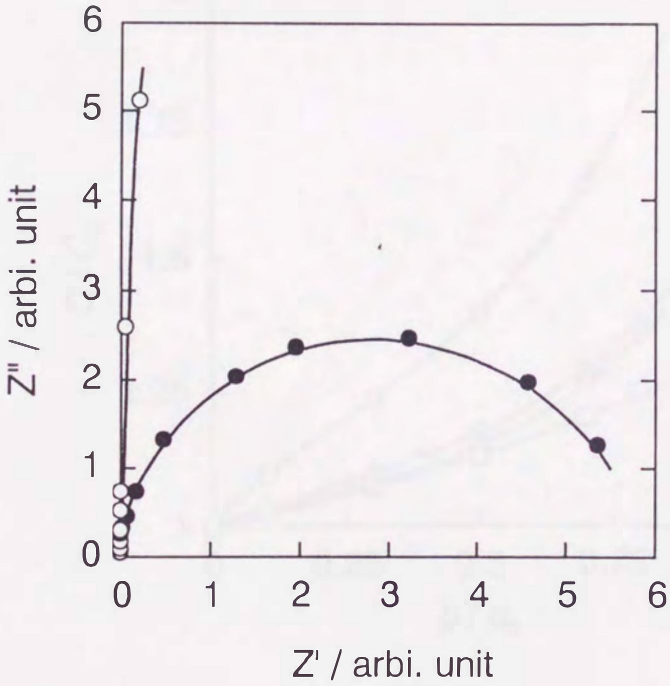

Fig. 14. Complex impedance plots for CA 39; (○) $p / p_0 = 0.4$, (●) 0.9.

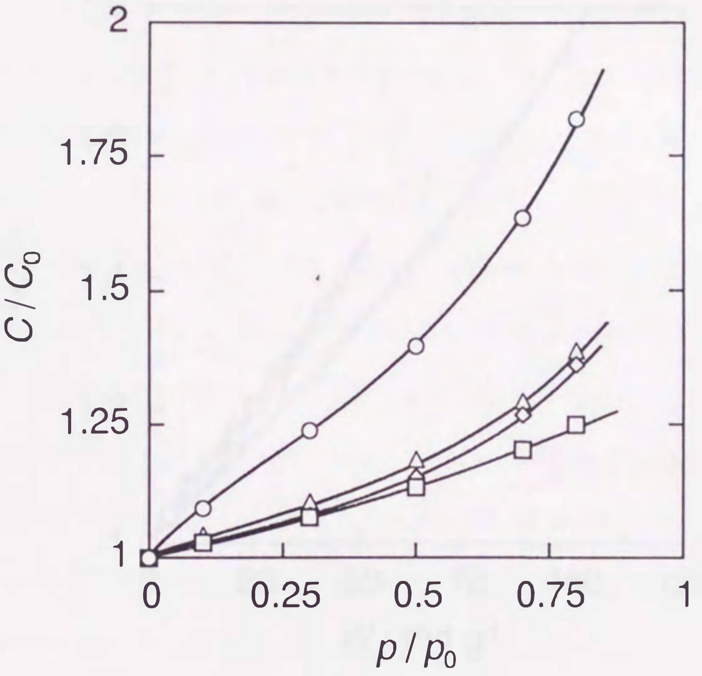

Fig. 15. Dependence of the capacitance on the relative vapor pressure at 30 ℃, 100 kHz; (○) CA 39, (△) CAP 48, (□) CAB 38 and (◇) EC.

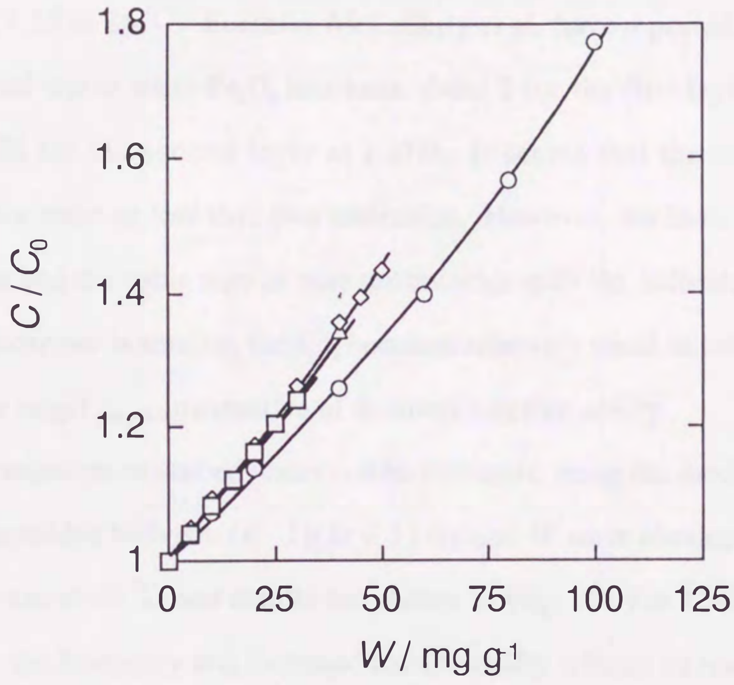

Fig. 16. Dependence of the C / C_0 on W at 30 ℃, 100 kHz;

(○) CA 39, (△) CAP 48, (□) CAB 38 and (◇) EC.

for CA 39. The relation seems to be derived from the different state of sorbed water.

In order to clarify the state of sorbed water, it is useful to estimate the dielectric constant of the sorbed water (ε_{H_2O}). We applied Kurosaki's equation (14), Eq. [10], to the result of Fig. 16. The value of ε_{H_2O} slightly increased with increasing the relative vapor pressure. The increment is due to the change of state of sorbed water from specific bound to loosely bound. The estimated values of ε_{H_2O} at 1 kHz were 25.6, 26.5, 24.5, and 26.9 at $p / p_0 = 0.8$ for the CA 39, CAP 48, CAB 38, and EC, respectively. As mentioned in Chapter II, the theoretical value of liquid water is 64 and that of single water molecule is 3.19 at 25 ℃. Further, McCafferty et.al. have reported (17-19) that the dielectric constant of adsorbed water on α-Fe_2O_3 had been about 2 for the first layer of physically adsorbed water and about 28 for the second layer at 1 kHz. It seems that the sorbed water in cellulose derivatives associate more or less than two molecules. However, we have to note that the evaluated ε_{H_2O} are mean value and the value may or may not coincide with the individual size of cluster. As the sorption ability of polymer is smaller, the ε_{H_2O} becomes relatively small in calculation. It is noteworthy that EC had slightly larger ε_{H_2O}, irrespective of its lower sorption ability.

Further, the polarization of sorbed water can be estimated using the modified Kirkwood equation, Eq. [8]. The relationships between $(\varepsilon - 1)(2\varepsilon + 1)/9\varepsilon$ and W were obtained at 1 kHz and 1 MHz in humidification process at 30 ℃ and results are shown in Fig. 17. For CAB 38, $(\varepsilon - 1)(2\varepsilon + 1)/9\varepsilon$ was not affected by the frequency and increased monotonically with an increase in W. This means that the intermolecular interaction of water-water and water-cellulose molecules are very weak. For CA 39, the distinction was observed in higher water content region. The difference between $[(\varepsilon_s - 1)(2\varepsilon_s + 1)/9\varepsilon_s - (\varepsilon_p - 1)(2\varepsilon_p + 1)/9\varepsilon_p]$ values observed at 1 kHz and 100 kHz approximates to the difference of $4N_2P$ (1 kHz) / 3 and $4N_2P$ (100 kHz) / 3 ($=\Delta P$) which indicates the degree of the orientation of dipoles of sorbed water. The results are summarized in Fig. 18. The ΔP values increased as the amount of sorbed water increased for all cellulose derivatives. In the lower sorption region, the value increased linearly with the sorbed water content, while the slope depended on the kind of cellulose

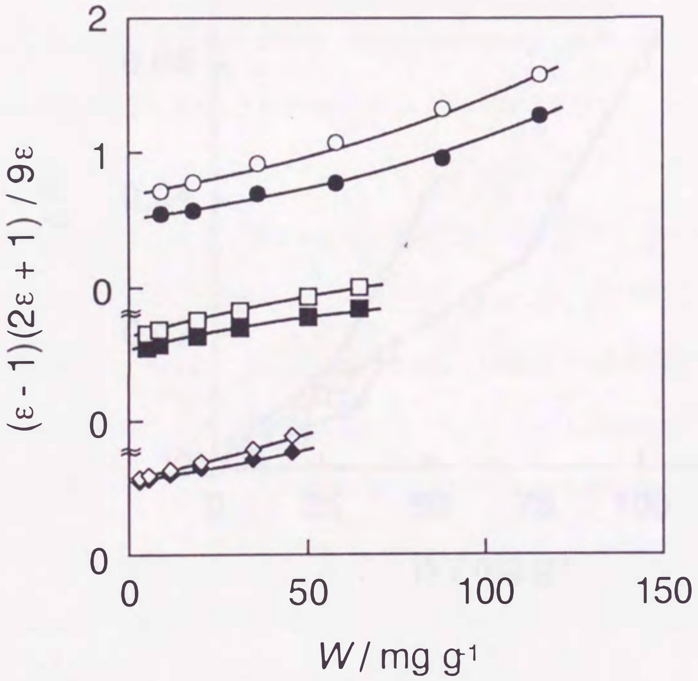

Fig. 17. Relationships between $(\varepsilon - 1)(2\varepsilon + 1) / 9\varepsilon$ and W at 30 ℃; (○) CA 39, (□) CAB 38 and (◇) EC; open: 1 kHz, closed: 100 kHz.

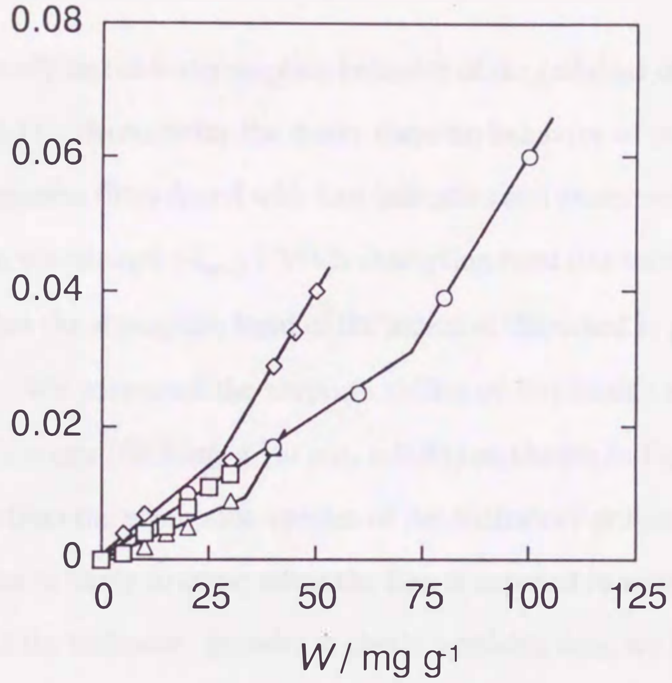

Fig. 18. Dependence of ΔP on W at 30 ℃;
(○) CA 39, (△) CAP 48, (□) CAB 38 and (◇) EC.

derivatives. This means that the state of sorbed water doesn't change in this region for each cellulose. However, ΔP increased steeply above a certain amount of sorbed water for CA 39 and EC. This inflection point seems to be related to the fact that formation of clusters of sorbed water starts. Especially, the value increased steeply even at low water contents for EC. The result is attributed to the higher tendency to cluster formation of EC and is consistent with the result obtained from sorption isotherm analysis.

3-3. Solvatochromic study on the water sorption behavior of the cellulose derivatives

As the third method to characterize the water sorprion behavior of polymers, we measured the UV/Vis spectra of composite films doped with four indicators and examined the effect of relative vapor pressure on the longest wavelength (λ_{max}) UV/Vis absorption band (the solvatochromic band).

It was observed that the absorption band of the indicator dispersed in polymer was influenced by the indicator content. We measured the sorption ability of Reichardt's betaine itself at first. The indicator sorbed much water (80.9 mg g^{-1} at $p/p_0 = 0.84$) as shown in Fig. 19 and this hydrophilic character is liable to affect the absorption spectra of the indicator / polymer composite. Further, the aggregation of indicator is likely to occur when the film is exposed to water vapor, particularly in the case of large content of the indicator. In order to obtain a reliable data, we have to note the quantity of indicator dissolves in the polymer. As expected, the smaller the content became, the less the influence. However, the absorption peak broadened and λ_{max} could not be assigned precisely under extremely low content. The effect of indicator content on spectrum was small for composite with indicator other than Reichard' s betaine. The determined optimum indicator contents were as follows; the weight ratio of polymer to indicator is 100 : 5 for indicator **1**, 100 : 5 for indicator **2**, 100 : 3 for indicator **3** and 100 : 2.75 for indicator **4**. On the basis of the results, subsequent discussion was carried out on the optimum composite film.

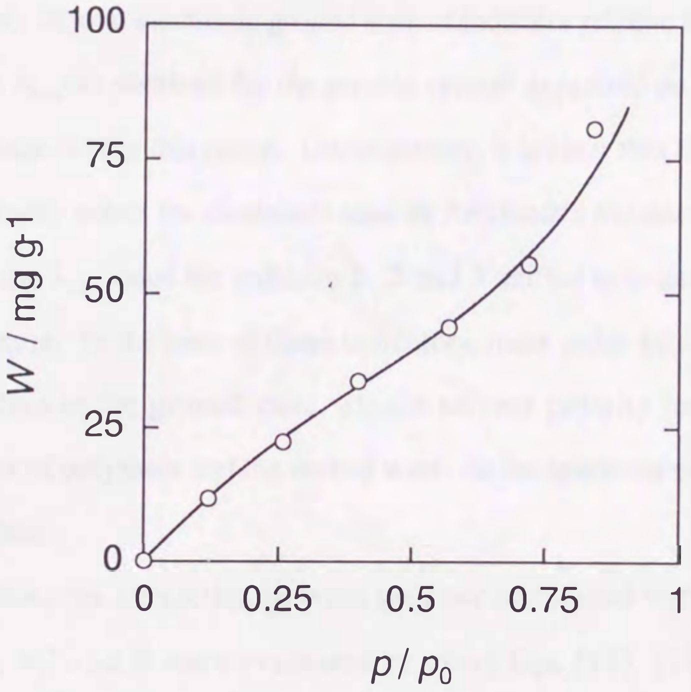

Fig. 19. Sorption isotherm of Reichardt's betaine dye measured at 30 ℃.

The typical UV/Vis absorption spectra observed for the composite films of Reichard's betaine **4** and CA 39 at various relative vapor pressure are shown in Fig. 20. It was observed that the absorption band is hypsochromically shifted with increasing the exposing relative vapor pressure. Other UV/Vis absorption data are listed in Table 1. It is known that the negatively solvatochromic pyridinium N-phenoxide betaine **4** exhibits one of the largest solvatochromic shifts; its longest-wavelength intramolecular charge-transfer (CT) absorption band is hypsochromically shifted by 357 nm on going from diphenyl ether (λ_{max} = 810 nm) to water (λ_{max} = 453 nm) as shown in Fig. 3. This is due to the stabilization of highly dipolar electronic ground state of indicator relative to less dipolar excited state in polar solvent. The λ_{max}(**4**) obtained for the present system depended on the polymer species and the relative vapor pressure within this range. Consequently, it is clear that the properties of polymer and the sorbed water greatly affect the electronic state of Reichardt's betaine as well as in solvent liquid. On the other hand, the λ_{max} value for indicator **1**, **2** and **3** shifted to larger wavelength with increasing relative vapor pressure. In the case of these indicators, more polar solvents stabilize the electronic excited states relative to the ground state. Hence solvent polarity leads to a bathochromic shift. However, the effects of polymers and the sorbed water on the spectrum of composite film of indicator **1**, **2** and **3** were a little.

In order to elucidate the interaction between polymer and sorbed water molecule, solvatochromic parameters, E_T, α, π_1^* and β were evaluated by using Eqs. [15], [19], [17] and [18]. All the parameters change with relative vapor pressure were shown in Figs. 21 - 24. It is noteworthy that there will be significant differences between the solvatochromic parameters for each cellulose derivatives.

These properties seems to be affected by the contents and the kinds of substituent groups. In order to reveal such effects, comparison of these parameters at dry atmosphere (p / p_0 = 0) with those of liquid solvents reported by Paley *et al*. seems to be useful (26). The present cellulose derivatives have hydroxyl group, various ester groups, and ethyl ether group as substituent groups. Consequently, we compared the parameters of cellulose derivatives with those of water, 1,3-butanediol, methanol, ethanol,

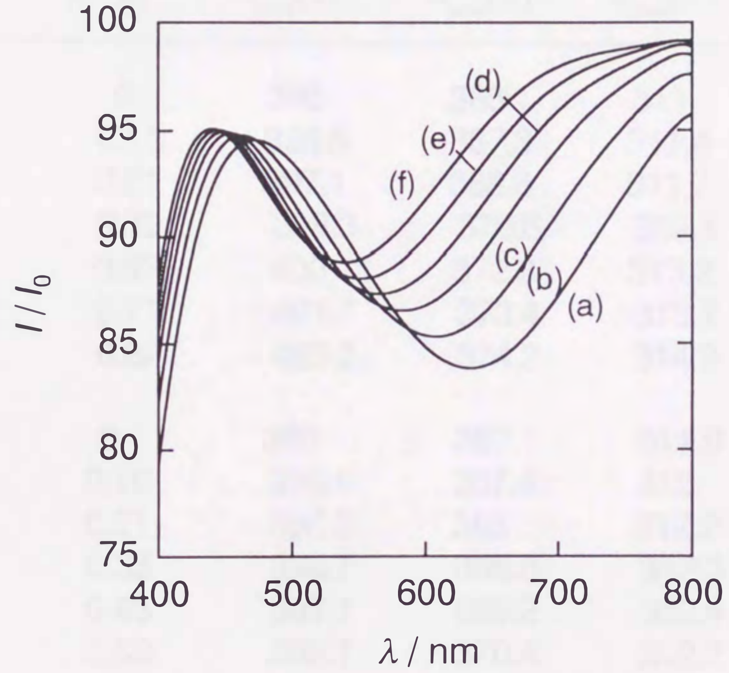

Fig. 20. The typical UV/Vis spectra for composite of Reichardt's betaine dye and CA 39; (a) $p / p_0 = 0$, (b) 0.12, (c) 0.3, (d) 0.46, (e) 0.61 and (f) 0.77.

Table 1-1. Absorption maximum of four dyes at various relative vapor pressure at 30 ℃.

Polymer	p/p_0	$\lambda_{max}(1)$	$\lambda_{max}(2)$	$\lambda_{max}(3)$	$\lambda_{max}(4)$
CA 39	0	396	366	311	638
	0.11	396.5	367.3	311.4	617
	0.21	397.1	368.6	311.7	599
	0.39	398.3	370.6	312.1	577
	0.57	400	372.3	313.2	560
	0.71	401.7	373.4	313.7	549
	0.82	403.2	374.2	314.2	542
CAP 48	0	396	367	311.9	641
	0.10	396.1	367.4	312	631
	0.21	396.3	368	312.2	619
	0.33	396.7	368.6	312.3	607
	0.43	397.1	369.2	312.4	599
	0.63	398.1	370.4	312.7	583
	0.79	399.1	371.4	312.9	572

Table 1-2. Absorption maximum of four dyes at various relative vapor pressure at 30℃.

Polymer	p/p_0	$\lambda_{max}(1)$	$\lambda_{max}(2)$	$\lambda_{max}(3)$	$\lambda_{max}(4)$
CAB 38	0	397	366	311.5	655
	0.16	397	366.5	311.5	638
	0.32	397.2	367.1	311.5	623
	0.47	397.4	367.8	311.5	611
	0.61	397.7	368.6	311.5	600
	0.73	398	369.5	311.5	592
	0.83	398.3	370.3	311.5	586
EC	0	384.1	360	305.7	722
	0.17	384.9	362.3	306	692
	0.31	385.6	363.6	306.3	674
	0.52	386.8	365.4	306.7	651
	0.67	388	366.5	307.1	638
	0.77	389	367.2	307.3	629
	0.80	389.3	367.4	307.4	627
	0.83	389.6	367.7	307.5	624

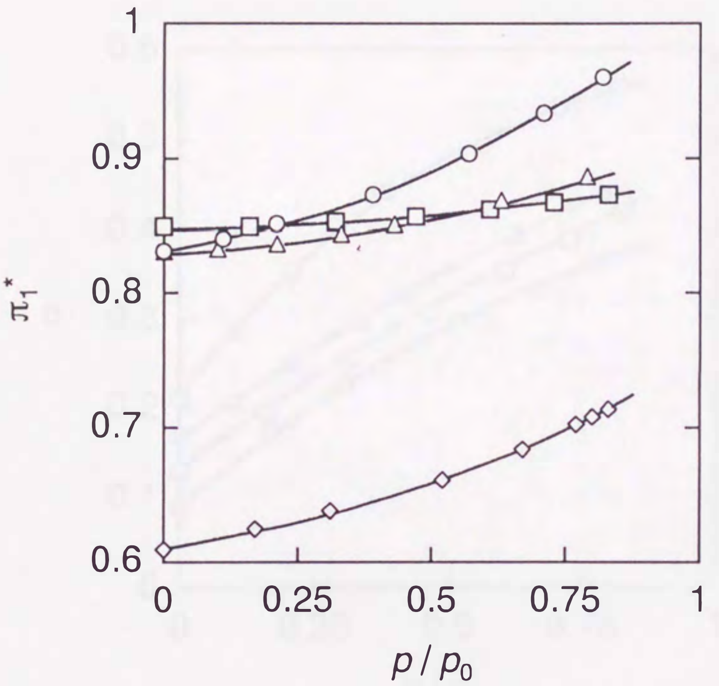

Fig. 21. Dependence of π_1^* on relative vapor pressure;
(○) CA 39, (△) CAP 48, (□) CAB 38 and (◇) EC.

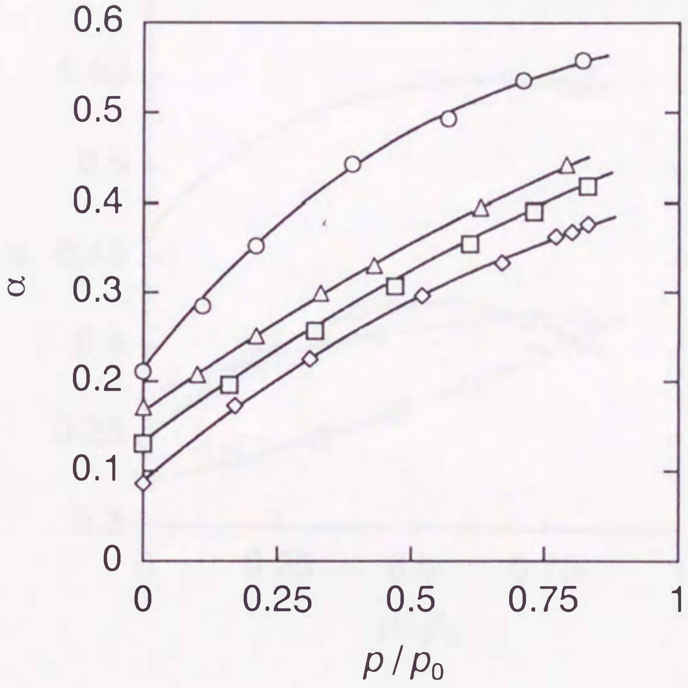

Fig. 22. Dependence of α on relative vapor pressure;

(○) CA 39, (△) CAP 48, (□) CAB 38 and (◇) EC.

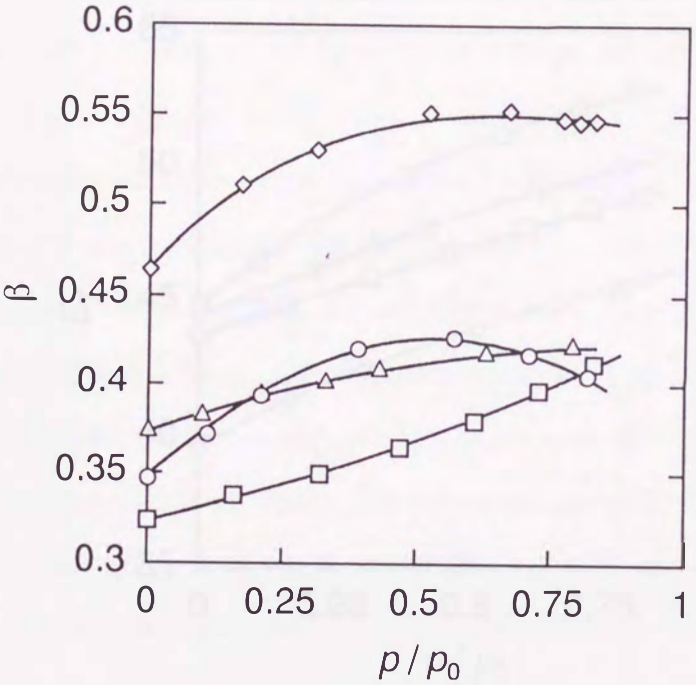

Fig. 23. Dependence of β on relative vapor pressure;

(○) CA 39, (△) CAP 48, (□) CAB 38 and (◇) EC.

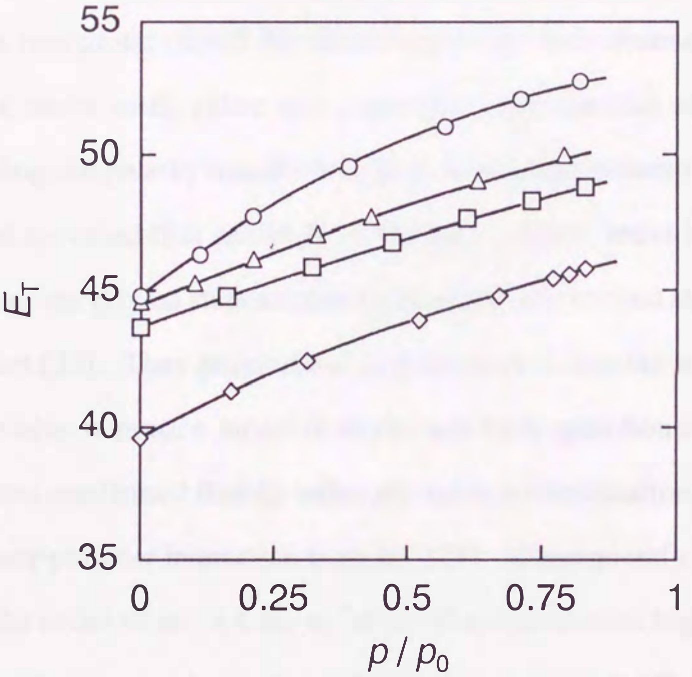

Fig. 24. Dependence of E_T on relative vapor pressure;

(○) CA 39, (△)CAP 48, (□) CAB 38 and (◇) EC.

methyl acetate, butyl acetate, and ethyl ether. In applying this methodology to characterize polymer, α shows the hydrogen-bond acidity of each polymer. In the case of cellulose derivatives, the groups that take part in hydrogen-bond acidity are considered as hydroxyl group for strong function and ester group for weak function. The values of α were fairly lower than those of *n*-alcohol (*ca.* 0.83-0.93) and 1,3-butanediol (0.66) for all cellulose derivatives. The values of α were also depended on the kind of cellulose derivatives, irrespective having similar hydroxyl group contents. This result suggest that, even if the polymer have protic group such as hydroxyl group, large constituent groups seems to act as steric factors and the polymer behave as less protic. CAB 38 which had large constituent group showed near-zero α value. The order of E_T value was almost the same as that of α. Taft *et al.* compared hydrogen bonding and polarity contributions to E_T differences between typical nonpolar and R-OH solvents and revealed that *ca.* 68 % of the total effect, must be attributed to preferential stabilization of the ground state relative to the electronic excited state by a specific solvent association effect (23). They pointed out as a result that, insofar as it is applied to protic solvents, the E_T value is more a measure of solvent hydrogen-bonding ability than polarity. Further, we also confirmed that E_T value represent a combination of non-specific (π_1^*) and specific (α) water-polymer interaction from Eq. [21]. Consequently, the order of E_T seems to be similar to the order of α. As for π_1^* scale, the values were higher than that of *n*-alcohol (*ca.* 0.5-0.6) and comparable to that of 1,3-butanediol (*ca.* 0.84) for all cellulose derivatives except for EC. It is noteworthy that EC has quite low value of π_1^*. It was observed that β value was small for cellulose derivatives and only EC had the value comparable to that of liquids with ether or ester groups (0.42-0.47). EC has a ether oxygen such as poly(ethylene oxide) which have sufficient electron-donating power (hard Lewis basicity). Consequently, it seems to be particularly hydrogen-bonded with Lewis acidic sites (hydroxyl group). In order to make sure the reason, we need further experiment.

As mentioned, we know that one of the most important factors, which affect water sorption ability, is the hydrophilicity of constituent groups of polymer. In attempting to understand the origins of differences in hydrophilic character, the relative numbers of atoms present in each polymer that might to be expected to form hydrogen bonds in water require consideration as well a polarity. However, polarity and/or hydrogen-bond acidity of polymers cannot be judged from the chemical structure or other analysis. In any event, the solvatochromic technique was able to reveal the difference of the characteristics of the polymer successfully, and these differences of properties of the polymer will be expected to reflect to the sorption behavior.

Next, we examined the water sorption behavior with a view point of molecular interaction by using above parameters. Figures 21-24 are replotted as the parameter change against the amount of sorbed water and shown in Figs. 25-28. Here, we have to give previous notice that the changes in λ_{max} with relative vapor pressure were small except for indicator 4 and the plotted parameters were estimated by interpolation. Although, the values of π_1^*, α and β might contain large errors in estimation, qualitative discussion could be done as follows. No relation between the values of these parameters obtained for dry film and water sorption abilities were observed. This result shows that the parameters of polymer does not offer a promising prospect of sorption ability. Instead of obtaining the reliable indication of the sorption ability of the polymer, it remained a possibility to reveal the interaction between polymer and sorbed water molecule and the state of sorbed water in the individual polymers. Water is well known as amphiprotic hydrogen bond acceptor-donor. Consequently, the state of sorbed water is expected to depend on the characteristics of the polymer such as polar groups. We discuss on the E_T which showed the large negative solvatochromism by sorbing water at first. The E_T value shifted to larger wavelength with increase in the amount of sorbed water for all polymers. These results indicate that the "polarity and/or hydrogen bonding ability" of the polymers becomes larger as they sorb water vapor from the atmosphere. This is reasonable since the

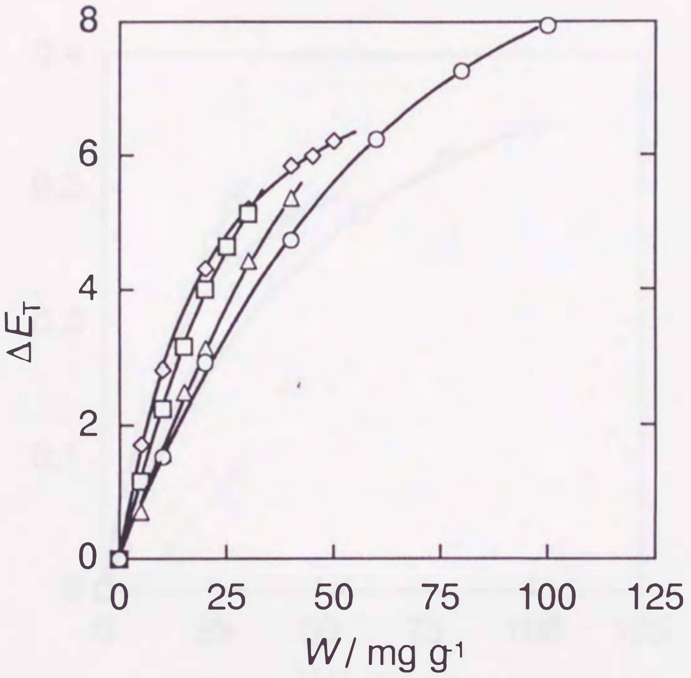

Fig. 25. Dependence of ΔE_T on W; (○) CA 39, (△) CAP 48, (□) CAB 38, (◇) EC.

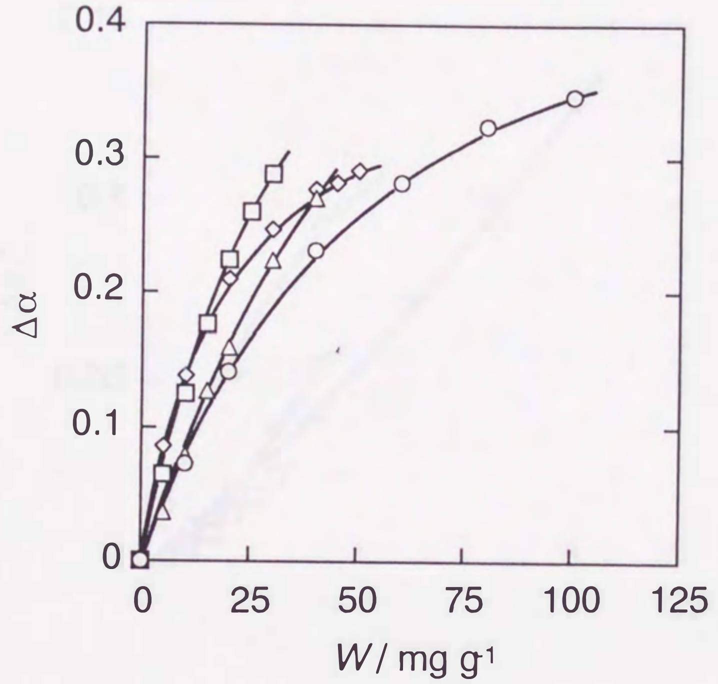

Fig. 26. Dependence of $\Delta\alpha$ on W; (○) CA 39, (△) CAP 48, (□) CAB 38, (◇) EC.

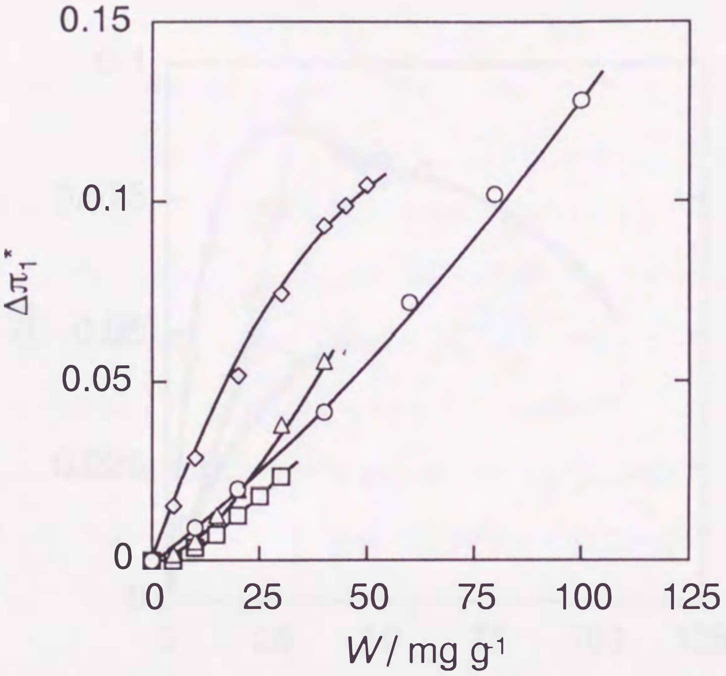

Fig. 27. Dependence of $\Delta\pi_1^*$ on W; (○) CA 39, (△) CAP 48, (□) CAB 38, (◇) EC.

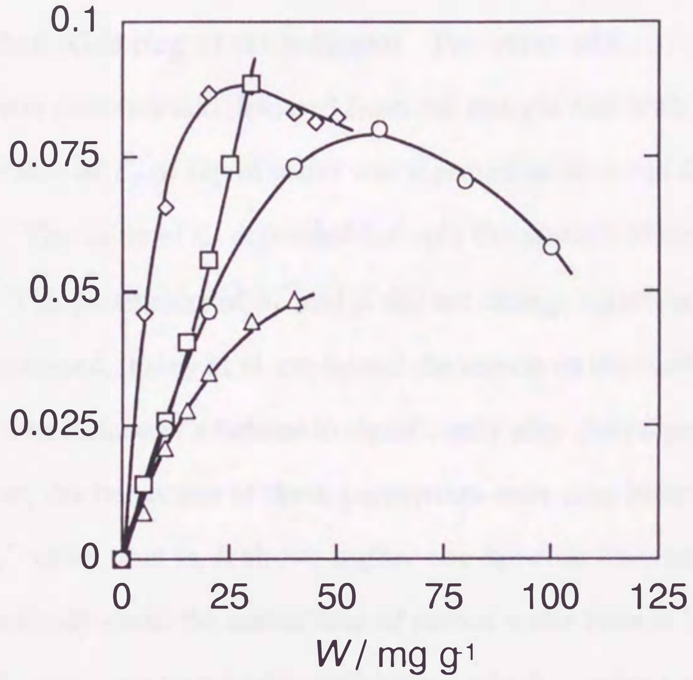

Fig. 28. Dependence of $\Delta\beta$ on W; (○) CA 39, (△) CAP 48, (□) CAB 38, (◇) EC.

presence of highly polar and amphiprotic water molecules in the polymer would be expected to enhance the "polarity and/or hydrogen bonding ability". The presence of sorbed water in the polymers also gave nonzero values of α. The result suggests that the sorbed water causes the hydrogen-bond acidity, that is, the oxygen of sorbed water in the polymer acts as a hydrogen-bond acceptor to acidic sites in the polymer framework. These hydrogen-bonded water molecules then act acidic sites. The hydrogen-bond acidity of this water causes the blue shift in the absorption of Reichardt's dye. The OH group of the water acts as a hydrogen-bond donor to the basic O^- on the phenoxide ring of the indicator. The value of E_T or α increased almost linearly in the low water contents and deviated from the straight line with further increase in water contents. The value of E_T of liquid water was reported as 63.1 and the curve gradually approached the value. The value of E_T depended not only the amount of sorbed water but also the cellulose species. The parameters of π_1^* and β did not change significantly upon exposure to water vapor as mentioned. Paley et al. explained the reason as the indicators **1-3** are less sensitive to moisture than Reichardt's betaine to significantly alter their dipolarity/polarizability and basicity. However, the behaviors of these parameters were also interesting. EC had the particularly large $\Delta\pi_1^*$ value, that is, it shows higher non-specific interaction (dipole-dipole interaction). This result may mean the association of sorbed water even at low water contents. As for CA 39, the value increased gradually with increase in the amount of sorbed water and the curve was concave downward above 50 mg g^{-1}. This is also related to the association of sorbed water. For further detailed discussion on behavior of $\Delta\pi_1^*$, we have to exclude the effect of hydrogen bonding by using the indicators which are neither hydrogen bond acceptors nor donors. The value of β increased initially for all cellulose derivatives in the low water contents region because of amphiprotic nature of water. The value of $\Delta\beta$ of sorbed water in EC had a larger value among the cellulose derivatives at the same water content. This seems to be due to the hydrogen bond accepting nature of EC as suggested from large β value in dried state. The hydroxyl group of sorbed water in the polymer acts as a hydrogen bond donor to strong basic sites, ether oxygen. In this case, sorbed water acts as hydrogen acceptor as well as hydrogen donor. Consequently, the absorption of hydrogen bond donating indicator shift. However, the value decreased above a certain amount of sorbed water for CA 39 and EC. The amounts of sorbed water that the curve showed maximum were 60 mg for CA 39 and 25 mg for EC, respectively. These inflection point seems to be related to the cluster formation of sorbed water molecule. The reported value of β of liquid water is quite small (0.18) and the β value of sorbed water approach the value as the sorbed water associate. Further, it is interesting that the amount of sorbed water correspond to the inflection points observed in solvatochromic method is quite similar to that observed in polarization measurement. Consequently, it was proved that the solvatochromic method was one of the effective techniques for clarifying the sorption behavior of less hydrophilic polymer.

5. Conclusion

In conclusion, the complementarity was confirmed between three different technique for predicting and explaining the sorption behavior of the cellulose. There are at least two dominant modes of sorption of water in cellulose film. The first mode occurs at lower sorbed concentrations and corresponds to the interaction of the water molecules with the polar hydroxyl group or less polar carbonyl and/or ether group in the amorphous regions of cellulose. The sorbed water on hydroxyl group seems to be highly bound and that on carbonyl or ether group seems to be loosely bound to polymer. When the specific sites are occupied, additional sorbed molecules of water tend to associate to form clusters. This sorbed water behaves as if vapor like water as shown in Fig. 1. The tendency to form the clustered sorbed water molecules was higher especially for EC, which have no apparent hydrogen-bond acidity. The size of cluster estimated from the dielectric measurement was small. The solvatochromic parameters were also quite sensitive to the presence of water in the polymers, especially for E_T and α. Only EC was characterized by a high hydrogen-bond basicity and the sorbed water molecule in EC acts as strong hydrogen-bond acceptor. Further, β parameter was effective for the elucidation of state of the sorbed water, because it increased first and decreased with the cluster formation started. The solvatochromic technique was proved to be a useful technique to elucidate the water sorption behavior in polymer in view of molecular interaction.

IV-II. Effect of the cross-linking structure of the methacrylate polymers on the water sorption behavior

1. Introduction

The molecular packing is one of the factors which affect on the water sorption behavior as well as hydrophilicity of the polymer. However, the water sorption of a polymer at a given temperature, based on its morphology, has not been properly understood.

It had reported that the cross-linking has produced a marked increase in water sorption in copolymers of methyl methacrylate and dimethacrylate (7-11). For copolymers of MMA with both ethylene glycol dimethacrylate (EGDMA) and triethylene glycol dimethacrylate (TGDMA), water sorption was found to increase with an increase in cross-linking (7). A similar conclusion was drawn independently, as an aside to other studies of proprietary cross-linked poly (methyl methacrylate) (8). D. T. Turner *et al.*, made the glassy cross-linked networks by copolymerizing of methyl methacrylate both with ethylene glycol dimethacrylate and with triethylene glycol dimethacrylate, using a redox initiator (9). The saturation value for water uptake increased with increasing feed of dimethacrylate to more than twice the value for the linear polymer, i.e., poly (methyl methacrylate). The reason for this trend is not revealed. The density of the product increased. C. R. Moylan *et al.* measured sorption of water vapor into thin films of a cross-linked dimethacrylate UV-cured polymer by means of a quartz crystal microbalance apparatus (10). On the other hand, Kalachandra *et al.* determined the water sorption ability by Karl Fischer analysis (11). The work compares the water uptake and contact angle measurements of four glycol dimethacrylate and eight normal methyl methacrylate monomers and polymers. The uptake of water depended on the oxygen content for the series of polymer. The diffusion coefficients (D) were generally lower for the networks based on difunctional methacrylates compared with methyl methacrylates, presumably because of the highly cross-linked nature of the former. It would be interesting to study the morphology of the materials to seek an explanation of this phenomenon.

The difference between the linear polymers and the cross-linked polymers are molecular packing, that is, the size of the free space around the polar site of polymer. In the case of hydrophobic polymers which have no strong sorption site, the free space likely to be important as sorption site. In the present study, cross-linked polymers which have carbonyl group as polar site were chosen. The state of sorbed water in the polymer film was investigated with dielectric measurement and quartz crystal microbalance (QCM) technique. Effects of the degree of cross-linking and of the chemical structure on the sorption behavior are discussed. Further, dependence of the amount of sorbed small solutes on the degree of cross-linking was investigated in order to obtain the microscopic information regarding the size of the free space.

2. Experimental

2-1. Materials

Two series of experiment were performed in this study.

In the first experiment, methyl methacrylate (Mitsubishi rayon) was used as primary monomers. Divinyl benzene (DVB), ethylene glycol dimethacrylate (ED, F.W. = 198.22), 1.3-butyleneglycol dimethacrylate (BD, F.W. = 226.28), triethylene glycol dimethacrylate (3ED, F.W. = 286.33), tetraethylene glycol dimethacrylate (4ED, F.W. = 330.38) and 1.3-butylene dimethacrylate (BD) were used as cross-linking agent. Chemical structure of these monomers are shown in Fig. 29.

In the second experiment, vinyl benzoate (VB), vinyl cinnamate (VCi), vinyl methacrylate (VM) and vinyl crotonate (VCr) monomers (Shinetsu Sakusan Vinyl) were used as starting monomers.

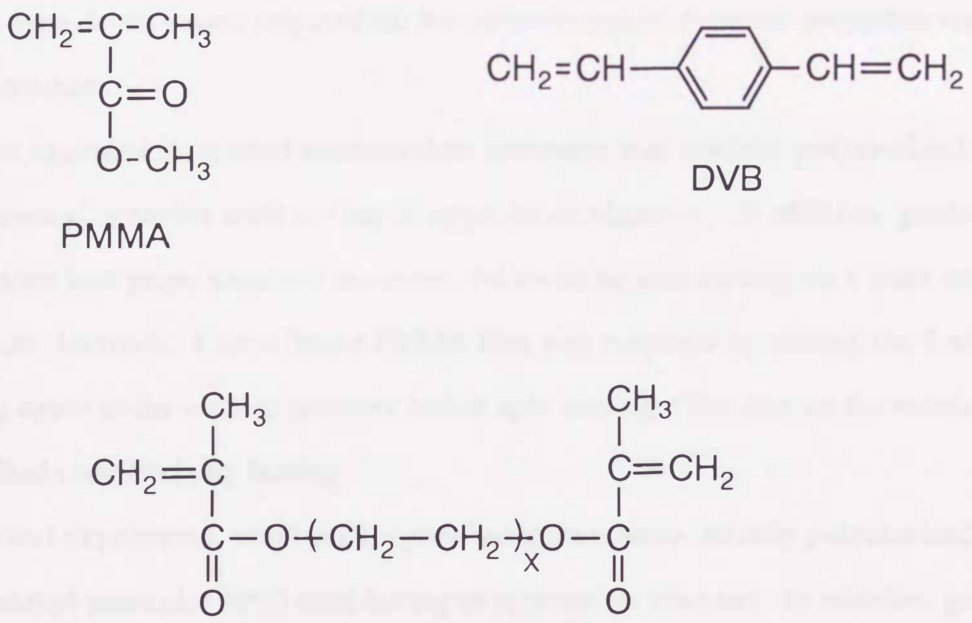

PMMA

DVB

x = 1: ED, 3 : 3ED, 4 : 4ED

Fig. 29. Chemical structure of MMA and cross-linking agent.

While VB has one double bond, others have two double bonds and the possibility to form a cross-linked film. Further, these monomers have a slightly different side group. The differences in the chemical structure of monomers are expected to form different chemical polymer structures. Chemical structure of these monomers are shown in Fig. 30.

2-2. Preparation of measuring device

Sandwich-type devices were prepared for the measurement of dielectric properties according to the following procedure.

In the first experiment, methyl methacrylate monomer was initially polymerized with a small amount of benzoyl peroxide until having an appropriate viscosity. In addition, graded amounts of BPO were added into prepolymerized monomer, followed by spin coating on a glass substrate which had a platinum electrode. Cross-linked PMMA film was prepared by adding the 5 weight percent cross-linking agent to the viscous polymer before spin coating. The film on the substrate was dried and polymerized completely by heating.

In the second experiment, vinyl carboxylate monomers were initially polymerized with a small amount of benzoyl peroxide (BPO) until having an appropriate viscosity. In addition, graded amounts of BPO were added into pre-polymerized monomer, followed by spin coating The film on the substrate was also dried and polymerized completely by heating.

The rest of procedure for preparing the device were already mentioned in CHAPTER III.

A thin polymer film was also formed on a quartz crystal oscillating element (4 MHz) with a silver electrode for determining the water content.

2-3. Measurement

The measuring method was already mentioned precisely in CHAPTER III.

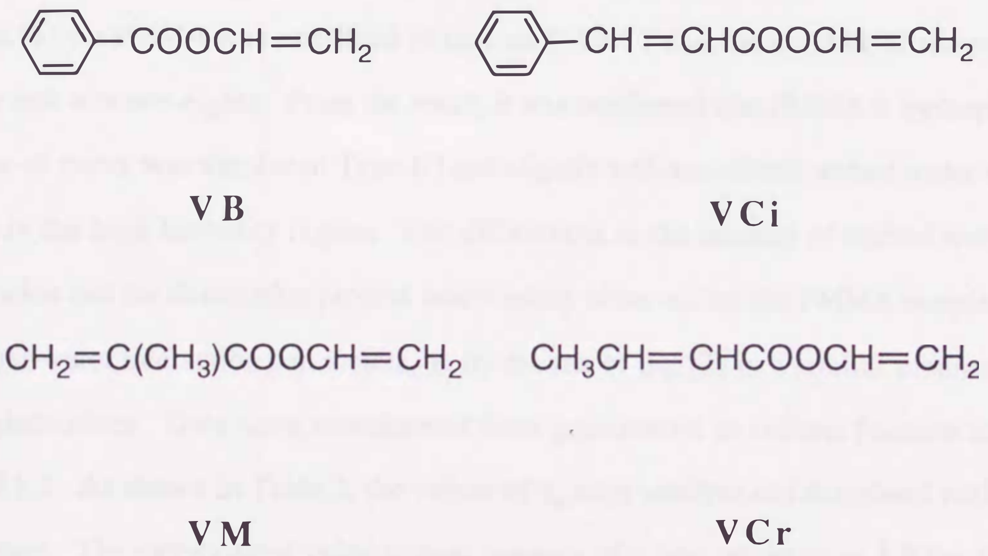

Fig. 30. Chemical structure of poly(vinyl carboxylates).

3. Results and discussion

3-1. Sorption behavior of water molecule on PMMA and cross-linked PMMA

3-1-1. Sorption isotherm of PMMA itself

Sorption isotherm was shown in Fig. 31. The amount of sorbed water on the PMMA thin film was *ca.* 25 mg/g at $p / p_0 = 0.9$ and this value corresponded to 0.14 water molecule per monomer unit. Comparing this result with some cellulose derivatives previously mentioned, the amount of sorbed water (wt.%) on PMMA was one-third of that on CAB 17 and the number of water molecules per monomer unit was one-eighth. From the result, it was confirmed that PMMA is hydrophobic polymer. The shape of curve was similar to Type III and slightly self-associated sorbed water molecules were expected in the high humidity region. The differences in the amount of sorbed water between the humidification and the desiccation process was scarcely observed for the PMMA sample. We estimated the polymer-water interaction parameters, χ, by means of Eq. [2] in a similar manner in the case of cellulose derivatives. Data were transformed from gravimetric to volume fraction using a polymer density of 1.2. As shown in Table 2, the values of χ, were positive and decreased with increasing the water content. The extrapolated value to zero pressure of χ was reported as 3.8 for PMMA (32). It seems that the results obtained in this study is reasonable value. Further, the clustering function developed by Zimm and Lundberg was also estimated. The calculated variations using Eq. 3 of the clustering function was also tabulated in Table 2 as a function of water volume fraction ρ_1. The clustering function G_{11}/V_1 is an increasing function of the water concentration from large negative value to large positive value. For an ideal solution where the solvent excludes its own volume to the other molecules of the same type but does not otherwise perturb their distribution, $G_{11}/V_1 = -1$; higher values of the clustering function show a trend of the solvent molecules to cluster. It seems that the sorption process changes progressively with increasing water content. The polymer which had low

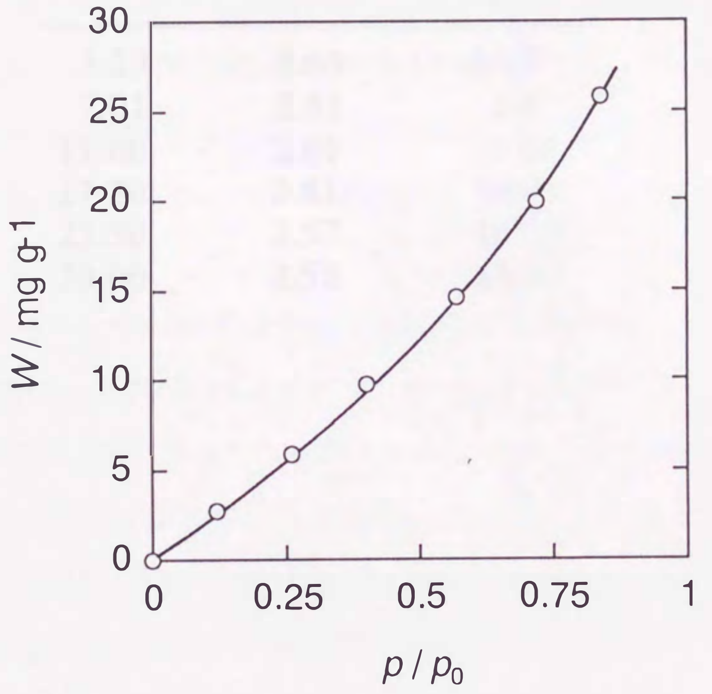

Fig. 31. Sorption isotherm for PMMA at 30 ℃.

Table 2. Data on PMMA calculated from the Eqs. [2] and [3] at 30 ℃.

$10^3\rho_1$	χ	G_{11}/V_1
3.29	2.60	-33.7
7.01	2.61	3.67
11.60	2.61	9.65
17.20	2.61	18.48
23.30	2.57	16.19
30.00	2.52	15.17

sorption ability showed a large negative value at extremely low water concentration. This is explained due to the small number of sorption site, not to the highly specific site same as the case of hydrophobic cellulose derivatives. Since hydrophobic polymer does not have highly specific sorption site, sorbed water molecules likely to become the sorption site. This explanation also holds for PMMA. PMMA has essentially highly trend for forming cluster of sorbed water in a higher p / p_0 region.

Cross-linked PMMA film is easily synthesized with some cross-linking agents having two vinyl groups. We prepared the cross-linked PMMA film on the substrate and also examined the sorption behavior of water on this thin film. There have been reported (8,9) that the saturation value for water uptake of PMMA increases with increasing degree of cross-linking. This behavior can be exhibited in terms of an increase in the concentration of the hydrophilic groups. However, the morphology of the materials should also be taken into consideration.

3-1-2. Dielectric measurement for PMMA and cross-linked PMMA

A complex impedance plot was used to analyze the results of impedance measurements because the impedance consists of resistive and capacitive components. As is distinct from the result of CA 39 shown in Fig. 14, only vertical line was observed for PMMA even at $p / p_0 = 0.9$ in the frequency range of 100 Hz to 1 MHz. This implies that the impedance can be approximated using $1/\omega C$ (ω is the applied angular frequency) and this device consists of an ideal capacitor.

The dielectric measurement was performed on cross-linked PMMA. The hysteresis was very small compared with that of cellulose derivatives. It was suggested that the origin for the hysteresis observed for cellulose was the formation of water molecule clusters, especially in a humid region. In the series of cross-linked PMMA, the formation of clusters hardly took place inspite of its high tendency to clustering. The hysteresis increased monotonously with an increase in the amount of sorbed water. In order to clarify the state of sorbed water, it is useful to estimate the dielectric constant of the sorbed water. We adopted Kurosaki's equation (14) , Eq. [10] in CHAPTER II. The estimated values of ε_{H2O} at 1 kHz was 25.0 at $p / p_0 = 0.9$ for PMMA. As mentioned in CHAPTER II, the dielectric constant of liquid water is 64 and that of unassociated water molecule is 3.19 at 25 ℃. Further, McCafferty et.al. have reported (17-19) that the dielectric constant of adsorbed water on α-Fe_2O_3 had been about 2 for the first layer of physically adsorbed water and about 28 for the second layer. The value of 25.0 is a little bit smaller than that of cellulose derivatives mentioned in CHAPTER II-II, 3-2. It seems that the mean values of association degree is less than two. Consequently, the interaction between polymer and sorbed water molecules or between water molecules was weak and the hysteresis became small. Further, the polarization of sorbed water was estimated using the modified Kirkwood theory, Eq. [8] in CHAPTER II. The subtracted values, ΔP, increased with the number of sorbed water molecules per monomer unit and led to 0.02 at $p / p_0 = 0.9$ for PMMA. The polarization became small compared with CA 39 or EC. Consequently, it can be said that the amount of sorbed water was too small to form cluster for PMMA and cross-linked PMMA. This result supports the previous discussion on the estimated ε_{H_2O} values.

The electrical capacitance changes at each relative vapor pressure depended on the cross-linking agent used as well as cross-linking temperature. The sensitivity over the relative vapor pressure range of $p / p_0 = 0$ to 0.9 ($C_{0.9} / C_0$) is shown in Fig. 32. When the PMMA was cross-linked at 90 ℃ for 1 h, the sensitivities became larger in the order of 4ED > 3ED > PMMA > ED ≥ BD > DVB. However, with increasing cross-linking temperature up to 170 ℃, the sensitivity is enhanced except for using the 4ED and resulted in similar value for all the cross-linking agent. This result is explained as follows. When the cross-linking temperature is low, cross-linking is insufficient as the length of the ether bond chain is long. Consequently, the unreacted cross-linking agent, which acts as a plasticizer, sorbs more water. As the cross-linking temperature increasing, the cross-linking was promoted and resulted in an increase in density of the polymer and in stiffness of the film. Consequently, the cause of increasing sensitivity by reacting at higher temperature seems to arise from its morphology, i.e., an increase in film stiffness leads to an increase in the free space for the sorption of water. We measured the film

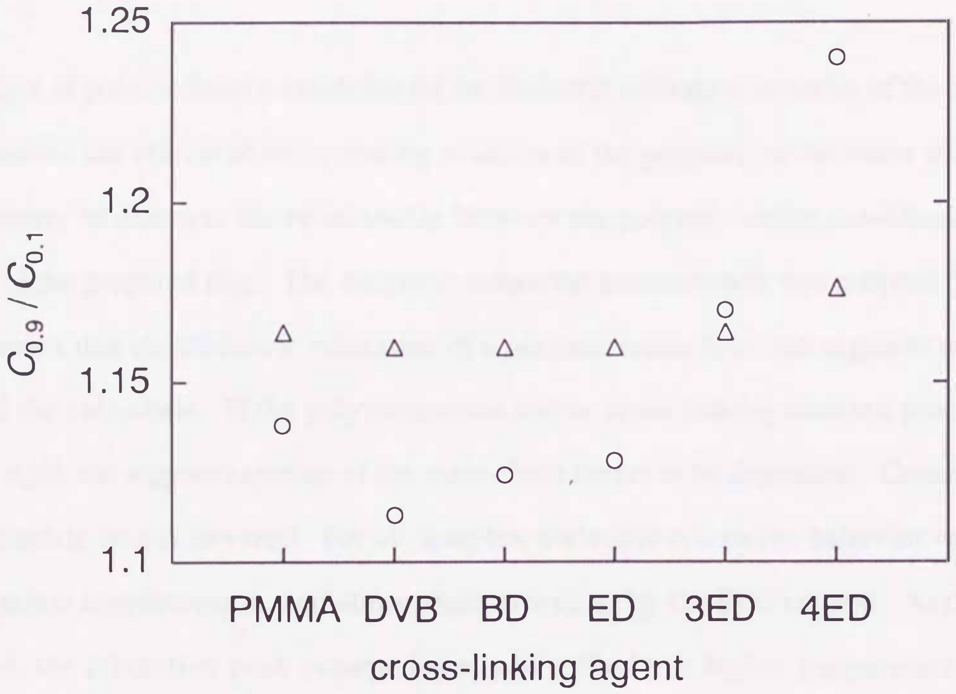

Fig. 32. Dependence of the sensitivity ($C_{0.9}$ / C_0) on the cross-linking agent and heating temperature for cross-linking; (○) cross-linked at 90 ℃ for 1 h, (△) 170 ℃ for 1 h.

thickness dependence of the amount of sorbed water on PMMA cross-linked with DVB. The amount of sorbed water per unit weight of cross-linked PMMA (mg/g) was independent of the film thickness (below ca.12 μm). It was also confirmed that the sensitivity of capacitance to relative vapor pressure change was independent of the film thickness. It is obvious that the sorbed water molecules on the film exist uniformly in the film.

3-2. Sorption behavior of water on the polymerized carboxylic acid vinyl esters

3-2-1. Effect of polymerization condition on the dielectric relaxation behavior of the film

To examine the effects of cross-linking structure of the polymer on the water sorption behavior, it was necessary to discover the relationship between the polymerization condition and the chemical structure of the prepared film. The dielectric relaxation measurement was adopted for this purpose. It is well known that the dielectric relaxation of a polymer arises from the segment motion of the main chain and the side chain. If the polymerization and/or cross-linking reaction proceeds and the film becomes rigid, the segment motion of the main chain seems to be depressed. Consequently, the value of the dielectric loss is lowered. For all samples, dielectric relaxation behavior was affected by the polymerization temperature, t_p, and atmosphere as well as by the BPO content. As the polymerization proceeded, the relaxation peak became lower and shifted to a higher temperature. In any case, the dielectric relaxation peak of the film polymerized in a nitrogen atmosphere was observed at a higher temperature compared with that in air. The peak height was also lowered by polymerizing in nitrogen. Effects of the polymerization temperature and the amount of BPO added to the pre-polymerized monomer on the value of tanδ and the temperature at maximum tanδ, t_{max}, are summarized in Table 3. Addition of 4 milligrams of BPO per gram of pre-polymerized monomer was effective to make the polymerization proceed. The effects of polymerization temperature were more complicated. Although the optimum polymerization temperature for obtaining film with the lowest value of tanδ depended on

Table 3. Polymerizing condition and some properties of the poly(vinyl carboxylate) films.

monomer	Sample No.	t_p °C	BPO mg g^{-1}	$\tan\delta \times 10^3$	t_{max} °C	schrinkage %
VB	1	90 (1h)	1	136.0	120	
	2	70 (1h)	1	48.6	90	
	3	70 (1h)	4	55.2	90	4.0
VM	4	120 (1h)	1	27.2	115	
	5	120 (1h)	4	21.3	115	11.3
	6	70 (1h) - 120 (1h)	1	23.0	120	
	7	70 (1h) - 120 (1h)	4	21.1	135	15.1
	8	90 (1h)	1	78.1	120	
VCr	9	70 (1h) - 120 (1h)	1	47.7	135	
	10	70 (1h) - 120 (1h)	4	17.5	155	
VCi	11	90 (0.5h) - 160 (1h)	1	165.5	210	
	12	90 (0.5h) - 160 (1h)	4	146.1	215	

the monomers used, the heat treatment in two stages was effective. It seems that the heat treatment at a lower temperature is related to the polymerization and that at higher temperature it is related to the acceleration of polymerization and the removal of the residual monomers. The tanδ vs. temperature relationships measured for the optimum films at 10 kHz are shown in Fig. 33. Especially, for the films obtained by polymerizing VM or VCr, the peak-height was very small. This behavior may be related to the cross-linking structure of VM and VCr because these compounds have two double bonds. Although VCi also has two double bonds, it is known that the cyclization is likely to occur in preference to the cross-linking reaction. Consequently, the dielectric relaxation peak did not decrease upon polymerization. It is natural that a linear polymer, VB, has a larger dielectric relaxation. Although we could not measure the degree of cross-linking directly, the order of the value of tanδ seemed to be equivalent to the order of the degree of cross-linking, that is, the polymer with higher degree of cross-linking structure showed a lower value of tanδ.

Change in film thickness with heat treatment was examined for VM. Results are shown as shrinkage percentage in Table 3. It can be observed that the film shrinks as the value of tanδ becomes lower. This is due to the proceeding of the cross-linking reaction and is consistent with the interpretation of the results of dielectric behavior. The measurement of the dielectric relaxation may be considered as a reliable indication of the degree of cross-linking.

3-2-2. Water sorption behavior of on the polymerized vinyl carboxylate thin films

The amount of sorbed water was measured for these polymer thin films as a function of relative vapor pressure, p / p_0. The effects of polymerization conditions on the amount of sorbed water were observed to be significant. The water content of the films W_g, which was based on grams of sorbed water per one gram of dry polymer, measured at $p / p_0 = 0.81$ and 30 °C is summarized in Table 4. It should be noted that the sorption ability increased with proceeding of the cross-linking reaction for each polymers. Sorption isotherms measured at 30 ℃ for the films are shown in Fig. 34. All the

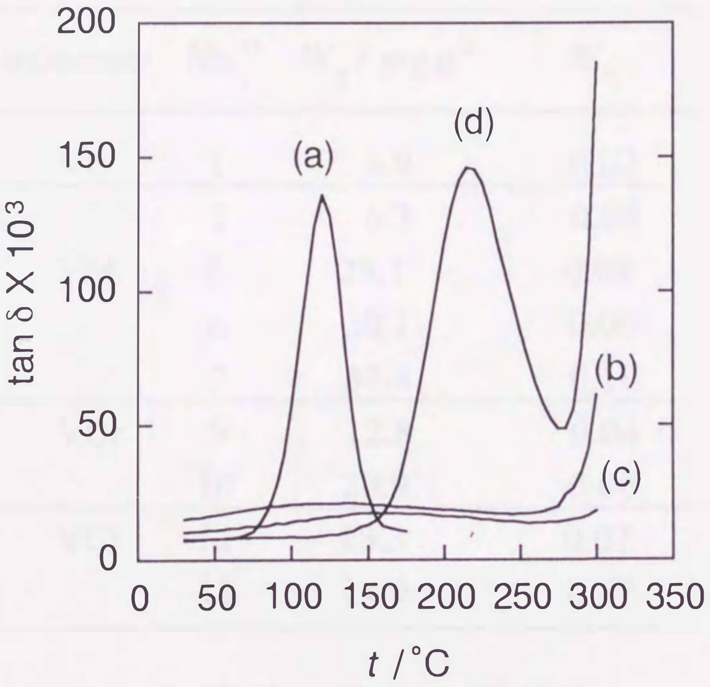

Fig. 33. Dependence of tan δ on temperature measured at 10 kHz;
(a) poly-VB (sample No.1), (b) poly-VM (No.7),
(c) poly-VCr (No.10) and (d) poly-VCi (No.12)

Table 4. The values of W_g and W_m measured at $p / p_0 = 0.81$ and 30 ℃.

monomer	No.[a)]	W_g / mg g^{-1}	W_m
VB	1	4.9	0.02
VM	2	6.1	0.04
	4	28.1	0.08
	6	30.1	0.09
	7	37.4	0.10
VCr	9	12.8	0.04
	10	20.9	0.06
VCi	11	13.3	0.07
	12	14.4	0.07

a) Sample No. is reffered to Table 3.

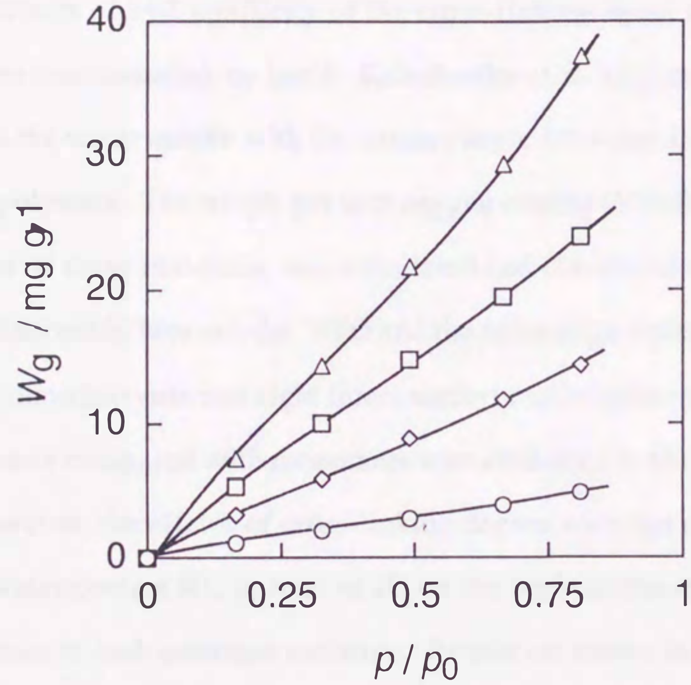

Fig. 34. Sorption isotherms measured at 30 ℃; (○) poly-VB (sample No.1), (△) poly-VM (No.7), (□) poly-VCr (No.10) and (◇) poly-VCi (No.12).

curves are almost linear. These polymers were hydrophobic and W_g depended on the polymer species. The differences of sorption ability seems to be derived from the differences of the structure of the films as well as the differences of the side groups of the polymer. It has been reported that the saturation value of water gain of copolymers of MMA with dimethacrylate monomers increases with increasing degree of cross-linking (7-10). The behavior can be interpreted in terms of an increase in the concentration of the hydrophilic groups by introducing the hydrophilic cross-linking agent. In the case of this system, the effects of hydrophilicity of the cross-linking agent need not to be considered because this monomer can cross-link by itself. Kalachandra et al. (11) measured the water sorption ability and compared the water uptake with the contact angle for water in glycol dimethacrylate and methyl methacrylate polymers. The weight per cent oxygen content (WPO), which is indicative of the hydrophilic character of these materials, was calculated and correlated with weight percent water uptake. The linear relationship between the WPO and the percentage water uptake was observed in a series of four glycol dimethacrylate and eight linear methyl methacrylate monomers. The increased water uptake of polymer compared with monomers was attributed to the microvoids present in the polymer matrix. However, the effects of cross-linking degree were not considered. We estimated another measure of water content W_m instead of W_g on the basis of the mole ratio of sorbed water molecule to oxygen atom in each monomer molecule. Results are shown in Table 4. Poly-VM had the largest W_m (0.10 mol water / mole oxygen atom) and decreased in the order of poly-VCr (0.07), poly-VCi (0.07), and poly-VB (0.04) at $p/p_0 = 0.8$. The value of W_m of the cross-linked polymers was greater than that of linear polymers. There were also some differences among the cross-linked polymers. These orders of W_m may be related to the cross-linking degree. The packing density change of the films with the formation of cross-linking structure should be taken into consideration. In the case of hydrophobic polymer without strong sorption site, the free space around the polar site is likely to be a sorption site. Cross-linked films prepared by polymerizing monomers with short chain seem to have highly strained chain conformations which prevent the close chain packing. That leads to an increase in free spaces. Now, it must be noted that the film shrinks as the cross-linking reaction proceeds, as shown in Table 3. The data seems to be in conflict with our explanation. However, the conflict may be resolved by the following explanation. A water molecule may be encompassed by a sphere of diameter about 3 Å, small enough to fit into typical microvoids or spaces that comprise the structural free volume. The volume, which was decreased by cross-linking reaction, seemed to be large compared with the adsorbate molecule (H_2O molecule in this case) and such a larger volume acted as dead volume for sorption in a hydrophobic polymer measured gravimetrically or electrically measurement. Consequently, the apparent reduction of volume in Table 3 was independent of results of the measurement of sorption ability. The free space we now consider as the sorption site is a molecular size in which the water molecule and polar site of polymer can interact. The space must affect the sorption behavior of the hydrophobic polymer. As mentioned above, the cross-linking reaction proceeds easily for VM and a lot of free space seems to exist. This explanation agreed with the order of water content.

In order to confirm the above discussion, the amount of sorbed water and the amount of sorbed methanol were measured for cross-linked VM. The van der Waals Volumes of these molecules can be calculated from the Bondi treatment as 11.49 cm^3 mol^{-1} for a water molecule and as 21.71 for a methanol molecule (4). Consequently, the size effect on the small molecules sorption ability of cross-linked polymer is expected to be revealed. As shown in Fig. 35, sorbed water in cross-linked polymer increased linearly with vapor pressure in this region. Here, the amount of sorbed molecules per monomer unit (VM monomer) is plotted on the ordinate. The result showed that the sorption of small molecules obeyed the Henry's law and the law was also expected to apply for the methanol sorption. The expectation seems to be true to a certain extent judging from the low sorption ability of the polymer. Further, the amount of sorbed water increased with increase in the degree of cross-linking at the same vapor pressure as mentioned above. Methanol molecule has a large dipole moment (μ = 2.87) compared with water molecule (μ = 1.85). If the sorption behavior is only governed by the

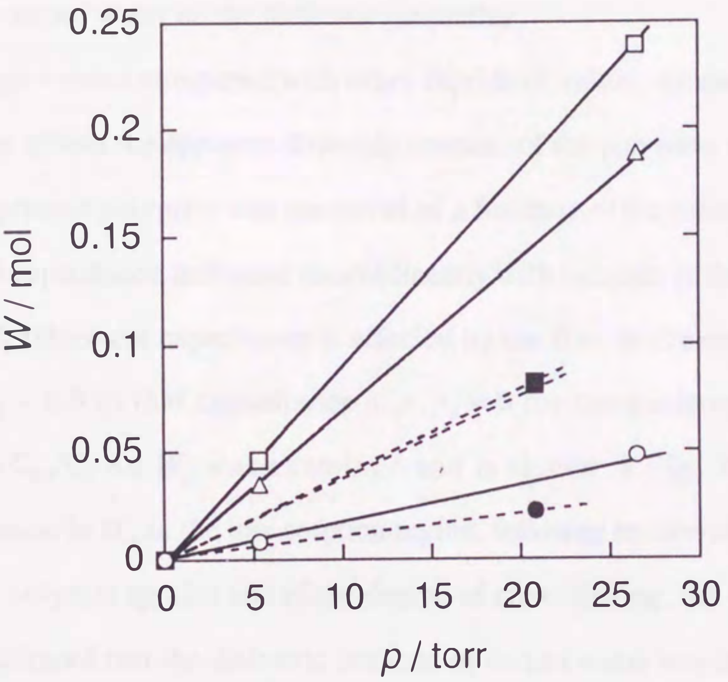

Fig. 35. Sorption isotherms of different solutes in poly-VM measured at 30 ℃; (○) Sample No.2, (△) No.6 and (□) No.7, ; open: water, closed: methanol.

dipole-dipole interaction, methanol must be more sorbed than water. However, the amount of methanol was small compared with water at the same vapor pressure. This result suggest that the sorption behavior of small molecules in the cross-linked VM is governed by the size of free space in the polymer as well as the dipole moment. Further, the amount of methanol no longer increased above a certain degree of cross-linking. This result also shows that the proceeding of the cross-linking reaction induced the small free space, which is effective only for water molecule sorption.

3-2-3. Effect of the sorbed water on the dielectric properties

Water has a large ε value compared with other liquids or solids. Consequently, the sorption of water in the polymer affects the apparent dielectric constant of the polymers very much. The electrical capacitance of the present polymers was measured as a function of the relative vapor pressure at 100 kHz. The electrical capacitance increased almost linearly with increase in the relative vapor pressure. The value of $C_{0.9}/C_0$ (since the capacitance is affected by the film thickness, we adopted the ratio of capacitance at $p/p_0 = 0.9$ to that capacitance at $p/p_0 = 0$ for comparison) are shown in Table 5. Dependence of the $C_{0.9}/C_0$ on W_g was examined and is shown in Fig. 36. The $C_{0.9}/C_0$ increased linearly with an increase in W_g in the low sorption region, followed by curvature upward. Irrespective of the difference of polymer species and of the degree of cross-linking, the $C_{0.9}/C_0$ depended only on W_g. This result implicated that the dielectric constant of sorbed water was the same in all the present polymers. The dielectric constant of the sorbed water was estimated by applying Kurosaki' s equation (14), Eq. [10]. The volume fraction of sorbed water was calculated from the amount of sorbed water assuming that the density of the polymers is 1.2 and that of water vapor is unity. The results are summarized in Table 6. The dielectric constant is less than that of liquid water, which is 76.6 at 30 °C, and also smaller compared with that of cellulose derivatives. The dielectric constant of sorbed water on cellulose derivatives had a larger value as mentioned in CHAPTER IV-II, 3-2. We have explained this behavior as the formation of clusters of sorbed water molecules. The value of the dielectric

Table 5. The value of $C_{0.9} / C_0$ measured at 100 kHz and 30 ℃ and the value of ε_ω estimated at $p / p_0 = 0.8$, 1 kHz and 30 ℃.

monomer	No.[a)]	$C_{0.9} / C_0$	ε_{H_2O}
VB	1	1.04	21.3
VM	2	1.05	20.4
	4	1.27	24.1
	6	1.30	24.9
	7	1.37	25.0
VCr	9	1.12	23.3
	10	1.33	34.5
VCi	11	1.13	24.3
	12	1.12	20.2

a) Sample No. is reffered to Table 3.

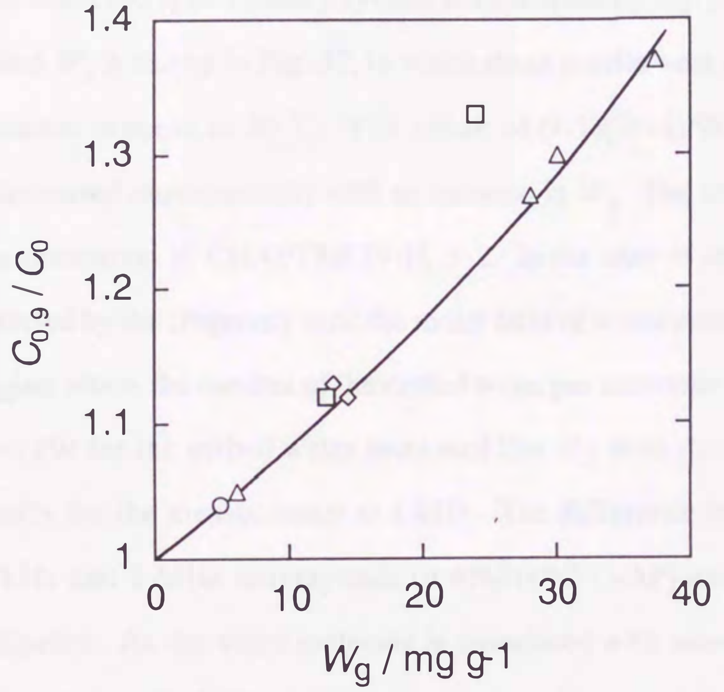

Fig. 36. Dependence of the $C_{0.9}$ / C_0 on the amount of sorbed water measured for film with various cross-linking degree at 100 kHz and 30 ℃; (○) poly-VB , (△) poly-VM, (□) poly-VCr and (◇) poly-VCi.

constant on these polymers is equivalent to the previously reported poly(methyl methacrylate) in CHAPTER IV-III, 3-1-2, which are too hydrophobic to form clusters. The dielectric constant became slightly larger with increases in the relative vapor pressure. This indicates that the interaction between water molecules becomes slightly larger and the sorbed water molecule begins to associate with increase in the amount of sorbed water.

Further the polarization of sorbed water was estimated. The modified Kirkwood's equation (18) for the dielectric constant, ε_0 of a binary system is expressed by Eq. [8]. The relationship between $(\varepsilon-1)(2\varepsilon+1)/9\varepsilon$ and W_g is shown in Fig. 37, in which these results were obtained at 1 kHz and 1 MHz in the humidification process at 30 °C. The value of $(\varepsilon-1)(2\varepsilon+1)/9\varepsilon$ was affected by the applied frequency and increased monotonically with an increase in W_g. The result is slightly different from that of cellulose derivatives in CHAPTER IV-II, 3-2. In the case of cellulose derivatives, the value was scarcely affected by the frequency until the molar ratio of water/monomer unit of cellulose became unity. In the region where the number of the sorbed water per monomer unit of cellulose was less than unity, $(\varepsilon-1)(2\varepsilon+1)/9\varepsilon$ for the sorbed water increased linearly with the amount of sorbed water then steeply, especially for the measurement at 1 kHz. The difference between $(\varepsilon-1)(2\varepsilon+1)/9\varepsilon$ values observed at 1 kHz and 1 MHz corresponds to $4N_2P(\omega)/3$ $(=\Delta P)$ and indicates the degree of the orientation of dipoles. As the water molecule is associated with more other water molecules with increasing W_g, the slope of $(\varepsilon-1)(2\varepsilon+1)/9\varepsilon$ vs W_g becomes larger and the differences of $(\varepsilon-1)(2\varepsilon+1)/9\varepsilon$ between two frequency becomes large. The value of ΔP at certain W_g at 30 °C is shown in Table 6. In the case of these polymers, the difference was very small compared with other polymers mentioned above. This is due to the small interaction between the polymers and the sorbed water molecules and between water molecules. By considering these results together with the result of estimated dielectric constant of sorbed water, the sorbed water scarcely formed clusters due to the hydrophobic nature and the space limitations of polymers.

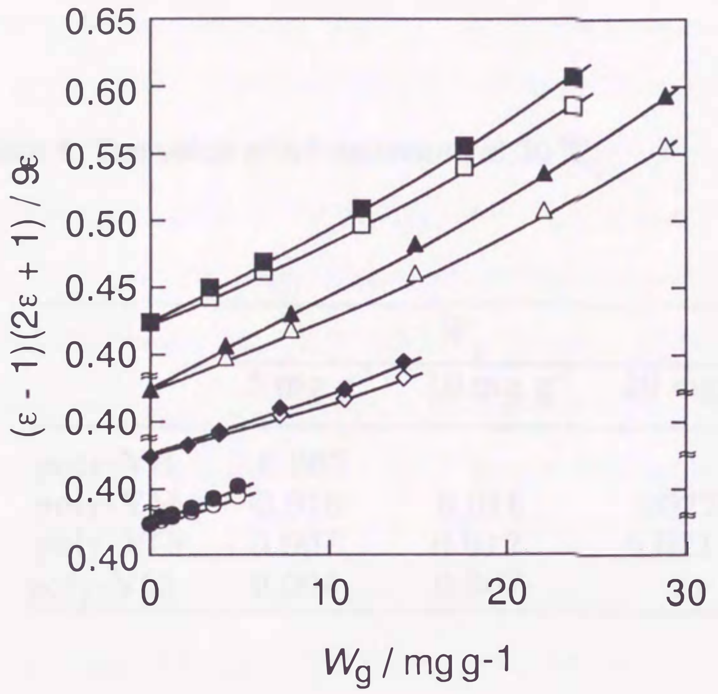

Fig. 37. Dependence of $(\varepsilon - 1)(2\varepsilon + 1) / 9\varepsilon$ on W_g measured at 30 ℃; (○) poly-VB (sample No.1), (△) poly-VM (No.7), (□) poly-VCr (No.10) and (◇) poly-VCi (No.12); open symbols: 100 kHz and closed symbols: 1 kHz.

Table 6. The value of ΔP estimated at 30 ℃.

	W_g		
	5 mg g^{-1}	10 mg g^{-1}	20 mg g^{-1}
poly-VB	0.007		
poly-VM	0.010	0.016	0.027
poly-VCr	0.007	0.012	0.021
poly-VCi	0.004	0.007	

4. Conclusion

It is well known that the most important factor which affect water sorption ability, is the polarity of constituent groups of polymer. However, other additional factors, such as molecular packing, must be considered, since the sorption site of water molecule seems to be the free space around the polar site of the polymer. In the respect of molecular packing, cross-linking structure is important as well as molecular weight. In fact, the cross-linked networks by copolymerizing methyl methacrylate with DVB, ED, BD and 3ED enhances the sorption ability. Some researchers have been reported that the increase of hydrophilicity by cross-linking induced the sorption ability. However, we showed that the sorption ability depended on the cross-linking condition as well as the cross-linking agent. Further, the sensitivity of electrical capacitance change with relative vapor pressure, which is related to the sorption ability, of the well cross-linked polymer hardly depended on the cross-linking agent. The sorption ability of the cross-linked polymer without using cross-linking agent were also examined. The difference of the structure of polymer, that is, whether the polymer was cross-linking type or linear type and the difference of the degree of cross-linking, affect the sorption ability. The polymer with highly cross-linked structure had a larger amount of water content. Consequently, the enhancement of water sorption ability by forming cross-linked structure is attributable to the increase in free space in molecular size around a polar site derived from the highly strained chain conformation. The state of sorbed water estimated with dielectric measurement was almost the same for both cross-linked and linear polymer, irrespective of the difference of degree of cross-linking. While PMMA had larger tendency to cluster formation of water (G_{11} / V_1 = *ca.* 15 in a higher p / p_0 region), the sorbed water molecules scarcely formed clusters. This can be explained because of the hydrophobic property and space limitation of the polymer. If the polymer is hydrophobic, it is difficult to diffuse the water molecule into the polymer. Even if the water molecule diffuse into the polymer, water molecule cannot form the cluster without existing enough spaces.